Building Research & Information

ISSN: 0961-3218 (Print) 1466-4321 (Online) Journal homepage: www.tandfonline.com/journals/rbri20

Extreme heat risk in retrofit cost–benefit analysis: probabilistic evaluation of overheating mitigation for mild climates

Tamara Lalyko , Diletta Ricci , Simona Bianchi & Alessandra Luna Navarro

To cite this article: Tamara Lalyko , Diletta Ricci , Simona Bianchi & Alessandra Luna Navarro (31 Oct 2026): Extreme heat risk in retrofit cost–benefit analysis: probabilistic evaluation of overheating mitigation for mild climates, Building Research & Information, DOI: 10.1080/09613218.2026.2746970

To link to this article: https://doi.org/10.1080/09613218.2026.2746970

© 2026 The Author(s). Published by Informa UK Limited, trading as Taylor & Francis Group

Published online: 31 Oct 2026.

Submit your article to this journal

Article views: 122

View related articles

View Crossmark data

Full Terms & Conditions of access and use can be found at
https://www.tandfonline.com/action/journalInformation?journalCode=rbri20

BUILDING RESEARCH & INFORMATION
https://doi.org/10.1080/09613218.2026.2746970

BRI Routledge Taylor & Francis Group

RESEARCH ARTICLE

OPEN ACCESS Check for updates

Extreme heat risk in retrofit cost–benefit analysis: probabilistic evaluation of overheating mitigation for mild climates

Tamara Lalyko[a], Diletta Ricci[b], Simona Bianchi[a] and Alessandra Luna Navarro[a]

[a]Department of Architectural Engineering and Technology, Delft University of Technology, Delft, Netherlands; [b]Department of Management in the Built Environment, Delft University of Technology, Delft, Netherlands

ABSTRACT

Despite the Netherlands' mild climate, heatwaves are becoming more frequent, and the use of mechanical cooling is rising, exposing the limitations of retrofit strategies designed primarily to reduce heating demand. While cost–benefit analysis (CBA) typically supports energy-efficient retrofits, it often overlooks rising cooling loads and the role of passive cooling measures. Consequently, stakeholders lack a long-term perspective on the financial implications of indoor overheating and the effectiveness of mitigation strategies under climate variability. This study proposes a probabilistic framework that integrates heat resilience into CBA by coupling building energy simulations with Monte Carlo risk aggregation to account for climate variability and extreme heat recurrence. The framework is demonstrated for a mid-century residential unit in Rotterdam over a 30-year historical reference period (1995–2024) by evaluating the Net Present Value of passive strategies (shading, high-albedo paint and their combination) and deep retrofit. The case study reveals a performance domain disparity, where passive measures reduce overheating intensity (53–59%) but yield only marginal cooling energy savings (2–6%). The study suggests that conventional CBA relying solely on energy savings underestimate the broader value of overheating mitigation, highlighting the need to consider thermal resilience and climate uncertainty in retrofit investment decisions.

ARTICLE HISTORY
Received 30 April 2026
Accepted 1 October 2026

KEYWORDS
Cost–benefit analysis; building retrofit; thermal resilience; heatwave; probabilistic risk assessment; passive cooling

Introduction

In recent years, an intense series of heatwaves has hit northern and western Europe, fundamentally shifting the region's climatic reality (C3S/ECMWF & WMO, 2026). Northwestern Europe has historically featured a mild climate, where heatwaves, as prolonged periods of unusually high temperatures, are now emerging as likely and seriously impactful hazards (KNMI, 2023; Taylor et al., 2023). This shift is part of a broader continental trend: Europe is warming faster than any other continent, with regional temperatures roughly 2°C above levels recorded fifty years ago (C3S/ECMWF & WMO, 2026). The severity of this warming became strikingly clear during the 2019 heatwave, which severely impacted countries with historically mild climates as temperatures hit 38.7°C in the UK and surpassed 40°C for the first time in the Netherlands (KNMI, 2023; Vautard et al., 2020).

Extreme outdoor air temperatures (>30°C) not only negatively affect labour productivity, but more critically, increase mortality rates, as evidenced by the 400 excess deaths a week during the 2019 heatwave in the Netherlands, which disproportionately affected individuals aged 80 years and older (Ebi et al., 2021; Reuters, 2019). During heatwaves, elevated outdoor air temperatures and solar radiation can induce indoor environments to excessively overheat, posing a critical risk to the health and well-being of occupants, particularly more vulnerable populations who spend their time indoors (NHBC, 2012; Spalt et al., 2016). To adapt to these escalating heat risks, building retrofits must be both resilient and financially feasible under future climate uncertainty. However, standard financial evaluations for retrofitting often rely on deterministic long-term average climate data, which fails to account for the unpredictability and severity of climate extremes (Sun et al., 2016). Therefore, integrating robust risk assessment into retrofit planning is fundamentally necessary. Without it, building stakeholders cannot reliably evaluate the true long-term financial feasibility or the functional resilience of adaptive measures across unpredictable future weather scenarios.

CONTACT Diletta Ricci d.ricci@tudelft.nl

© 2026 The Author(s). Published by Informa UK Limited, trading as Taylor & Francis Group
This is an Open Access article distributed under the terms of the Creative Commons Attribution License (http://creativecommons.org/licenses/by/4.0/), which permits unrestricted use, distribution, and reproduction in any medium, provided the original work is properly cited. The terms on which this article has been published allow the posting of the Accepted Manuscript in a repository by the author(s) or with their consent.

The paper proposes a novel framework that integrates climate uncertainty into the financial assessment of energy-efficient retrofits. Using a Monte Carlo simulation, this framework explicitly operationalizes heat extremes and propagates them into risk metrics. The main contributions of this approach are twofold: (i) integrating multi-year probabilistic heat hazard to evaluate their impacts across both energy performance and thermal comfort domains, (ii) translating resilience improvements into quantifiable cost savings to determine their financial viability within the cost–benefit framework. First, the research background is presented to highlight the existing gaps that motivate the proposed approach. The methodology for integrating heat hazard probabilistic modelling into retrofit strategies is then developed and reported in Section 2, followed by its demonstration through a case study in a temperate climate in Section 3. Finally, Section 4 discusses the applicability, limitations and future research directions of the proposed approach, while Section 5 presents the main conclusions.

Research background

As heatwave frequency, intensity and duration continue to increase under a changing climate, mild and temperate climates are facing new heat extremes (Krelling et al., 2024; Liyanage et al., 2024). Despite this shift, current retrofit strategies in these regions heavily prioritize winter insulation to cut heating costs and emissions, which can inadvertently trap heat and increase summer vulnerability, leading to maladaptation. Hamdy et al. (2017) found that residential typologies featuring large, glazed areas, limited solar protection, and insufficient ventilation are especially prone to overheating. Even within temperate climates, newer studies increasingly show that insulation-first retrofits can raise summer overheating risks unless shading, ventilation or other summer measures are included (Ibrahim & Pelsmakers, 2018; Liyanage et al., 2024; Yu et al., 2026).

To counteract these risks, modern retrofit strategies must be grounded in the concept of resilience, defined as 'the ability to prepare and plan for, absorb, recover from, and more successfully adapt to adverse events' (National Research Council, 2012). When applied to heat hazards, resilience relates to maintaining functionality in terms of thermal comfort or safety in indoor environments (Hong et al., 2023). Thermal resilience therefore spans two interconnected domains: energy demand and indoor thermal comfort. The energy demand domain encompasses the additional loads placed on cooling systems to prevent overheating, utilizing metrics such as energy use intensity, utility cost, and expected carbon loss (Bianchi, 2023; Lee et al., 2024). Conversely, indoor thermal comfort is assessed via thermal metrics counting the time and intensity of overheating, relying on indicators like the heat index, hours in heat stress, and the indoor overheating degree (Hamdy et al., 2017; Lee et al., 2024; Mirzabeigi et al., 2023; Sheng et al., 2023). Although these metrics provide a comprehensive assessment of thermal resilience, they are applied in performance evaluations rather than investment appraisal. As a result, improvements in thermal resilience are often treated separately from the economic analyses that ultimately inform retrofit decisions.

In identifying effective adaptation strategies to achieve this thermal resilience, research has examined both active and passive mitigation measures. While mechanical cooling offers an immediate intervention, an exclusive reliance on active systems is increasingly considered inadequate due to its energy intensity and vulnerability during power outages (Ebi et al., 2021). Consequently, the literature emphasizes the benefits of passive design measures, such as cool coatings for walls and adaptive solar shading, to reduce cooling energy loads and provide resilience in the event of system failure (Lee et al., 2024; Sheng et al., 2023). The strongest recurring recommendation is a combined strategy, integrating envelope measures with shading, ventilation, fans, reflective surfaces or efficient cooling, to maintain comfortable conditions when passive measures alone are insufficient (Le et al., 2025; Zhang et al., 2021).

When selecting among such adaptive retrofit approaches, recent studies employ Cost–Benefit Analysis (CBA) to systematically compare alternative retrofit packages by monetizing long-term benefits, such as energy savings and carbon emission reductions, against implicit costs (Sharbaf & Schneider-Marin, 2025). To building stakeholders, these financial implications play a decisive role in the adoption of adaptation measures, particularly under budget constraints (Ricci et al., 2025; Ruparathna et al., 2017). For estimating potential savings, standard CBAs rely on deterministic, long-term average climate data using Typical Meteorological Years (TMY), which may diverge substantially from actual outcomes as climate variability increases (Sun et al., 2016). This reliance on average weather conditions presents a limitation for heat adaptation retrofit appraisal, as the effectiveness of these measures is largely determined by extreme conditions. Consequently, deterministic CBAs may fail to capture the full economic value of adaptation measures and the financial uncertainty associated with heatwave occurrence.

To address climate uncertainties and accurately quantify hidden financial impacts, the European

Commission (2015) advocates for probabilistic risk assessment methodologies. Instead of static averages, a probabilistic financial assessment calculates how each parameter is distributed, often approximating potential outcomes via Monte Carlo simulations to reveal the true risk of non-profitable outcomes. A few studies have already shown the potential of risk assessment methodologies using heat wave projections and varying intensities of global warming (Hyyrynen et al., 2025; Sun et al., 2016). Applied to building performance, Sun et al. (2016) developed a probabilistic method of risk assessment for the calculation of EUI. Expanding this methodology to acute hazards, for example, Hyyrynen et al. (2025) demonstrated the use of probabilistic climatic inputs to evaluate the economic viability of active cooling to mitigate growing heatwave mortality risks, although their analysis was limited to the city scale. To fully capture the value of heat adaptation strategies, economic appraisal frameworks must move beyond one-sided energy billing and incorporate avoided overheating, outage resilience, health co-benefits and the uncertainty associated with future climate impacts. Developing such integrated probabilistic cost–benefit approaches remains an important research need (Brogno et al., 2025; Krelling et al., 2024; Lee et al., 2024).

Methodological approach

This study advances retrofit CBA by integrating probabilistic heat hazard modelling into financial risk assessment, to capture the variability and recurrence of extreme heat events. The approach links heat-related changes in cooling energy costs with retrofit economic performance, providing a basis for evaluating resilience under climate uncertainty.

The workflow comprises three interconnected stages (Figure 1). Stage I analyses historical climate data to derive a probabilistic characterization of heat hazard. These data inform dynamic energy simulations in Stage II, estimating performance variability under recurring extreme conditions. In both stages, thermal resilience is evaluated by: (i) considering the related cooling energy demand required to maintain acceptable thermal conditions, and (ii) the use of overheating metrics to define 'annual extremes'. Finally, in Stage III we applied CBA, by using cooling energy demand distributions as input for financial risk assessment. This cost modelling enables to convert energy demand variability into savings distributions, while Monte Carlo simulations are used to aggregate uncertainties and quantify overall financial risk under both average and worst-case hazard recurrence scenarios (see Section 0). The next subsections explain in detail each of these stages.

Stage I: climate data analysis

The initial stage assesses the occurrence and impact of extreme heat events to understand their relevance within the long-term perspective required for cost–benefit analysis. The study uses 30 years of historical weather data (1995–2024) from the Rotterdam Airport weather station, provided by the Dutch Meteorological Institute (KNMI, n.d.). This dataset captures observed climate variability and the empirical frequency of extreme events needed for probabilistic modelling but excluding future weather scenarios.

Daily temperatures are analysed to identify heatwaves and annual thermal intensity using established KNMI definitions. A heatwave is defined as a period of at least five days with maximum temperatures of 25°C or higher, including at least three days reaching 30°C (measured at the De Bilt station) (KNMI, 2023). Furthermore, thermal duration and intensity are quantified using degree-days with a 25°C threshold for summer days. All thirty years of the selected datasets are evaluated to identify which years featured extreme heat hazard or were characterized by thermal loads higher than average.

The impact of heatwaves on annual cooling performance is subsequently investigated through dynamic simulations. The analysis identifies the probabilistic range and threshold values for 'annual extremes' within the cooling energy domain (see Section 0). These definitions are essential for identifying the extreme years likely connected to hazardous events during building performance, for use in financial risk assessments.

Probability density estimation

Continuous variables such as annual energy demand and cost are modelled using Probability Density Estimation (PDE) derived from the 30-year dataset. Rather than fitting standard normal distributions, the nonparametric Kernel Density Estimation (KDE) method is used to generate a composite function to accurately represent irregular data frequencies (Weglarczyk, 2018). Physical consistency is ensured by constraining the bandwidth and excluding samples outside observed logical bounds. The resulting Probability Density Function (PDF) is subsequently converted into a Cumulative Distribution Function (CDF) for percentile analysis.

For this study, a simplified PDE approach is used to reduce the computational effort for the case study retrofit scenario assessment. Using the baseline PDF, a subset of seven reference years is selected to represent specific cumulative probabilities at the 0th, 5th, 25th,

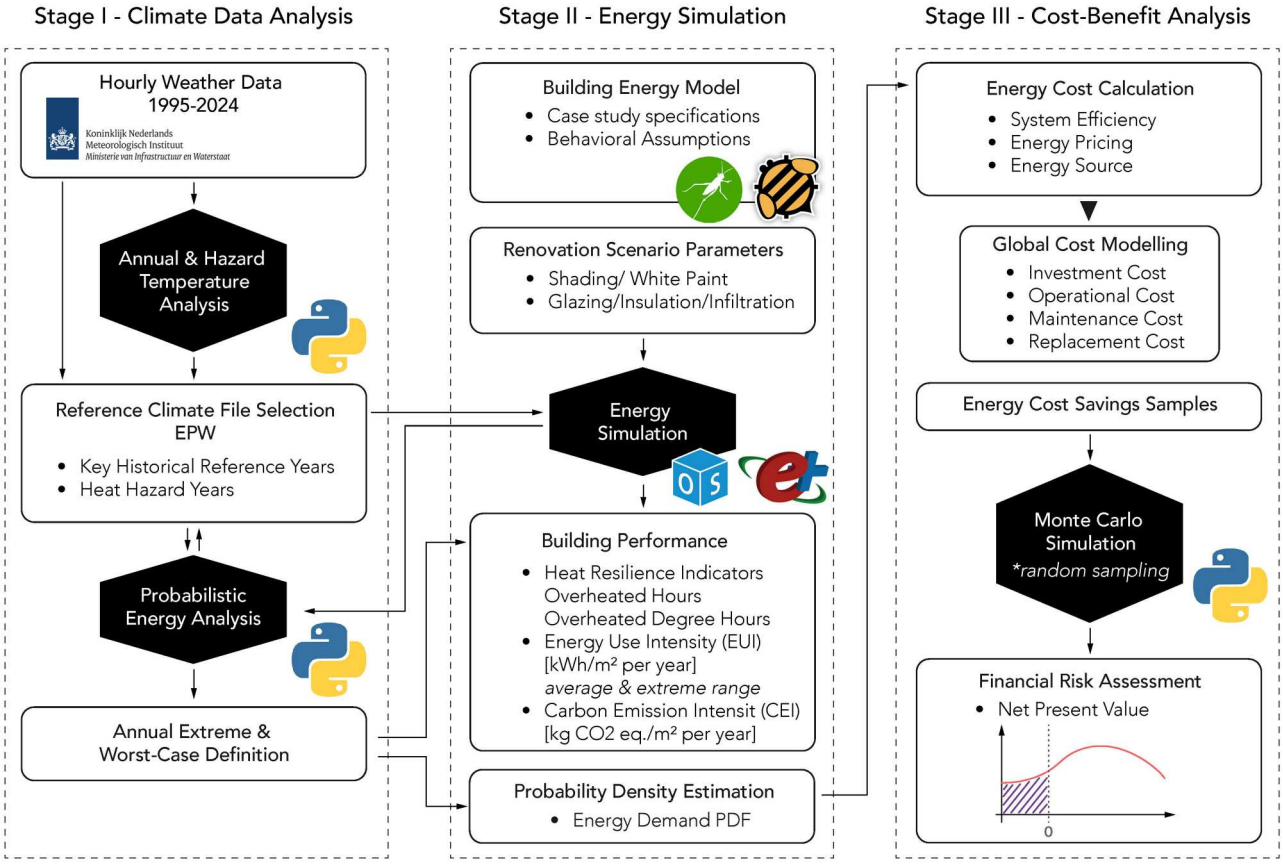


Figure 1. Overall workflow of the study: (a) climate data analysis to characterize extreme heat scenarios; (b) energy simulation to assess performance variability and thermal resilience; and (c) cost–benefit analysis using probabilistic demand and Monte Carlo simulation to quantify financial risk.

50th, 75th, 95th, and 100th percentiles, to capture low, typical and extreme years. The historical years most closely aligning with these thresholds serve as simulation inputs for all case studies (as-built vs. retrofit options). Finally, the results from these seven years are mapped to their respective probabilities and interpolated to reconstruct a simplified CDF, from which a new PDF is derived for each scenario.

Stage II: energy simulation

Building performance indicators

To quantify energy use and overheating, key performance indicators (KPIs) are defined and assessed to evaluate retrofitting objectives. As energy use is the key parameter in the CBA, overheating comfort metrics serve as a cross-comparison between monetary and occupant comfort value.

(a) Energy Use Intensity (EUI)

$$EUI = \frac{Demand\ (kWh) * EER}{Area\ (m^2)} \tag{1}$$

For the energy domain, the universally applicable indicator energy use intensity was selected, defined as energy use per square metre per year (kWh/m²) (Appendix A, Table A.1). Both the energy supply system's efficiency rating (*EER*) and the conditioned floor area are required in the quantification.

For overheating, two indicators were adopted to quantify both duration and severity. A fixed comfort limit of 28°C 'Standard Effective Temperature' (SET) was chosen (Huizenga et al., 2024). The temperature metric SET describes human temperature perception more accurately by including also mean radiant temperature, air speed, clothing and metabolic rate (ANSI/ASHRAE, 2017).

(b) Overheated Hours (OH)

$$OH = \sum_{i=1}^{N} 1_{(SET_n > T_{lim})} \times \Delta t \tag{2}$$

where,

- n is the integer representing the current calculation step (hour)

- N is final index for the simulation period
- SET_n is the simulated SET value for the specific time step (n)
- T_{lim} is the fixed upper temperature limit for thermal comfort
- Δt is the duration of each simulation step (for hourly data $\Delta t = 1$).

The metric counts the number of hours above the fixed comfort limit (T_{lim}) for the simulated period. The hour counts as 1 if the hour's specific SET value (SET_n) is larger than T_{lim}.

(c) Overheated Degree Hours (ODH)

$$ODH = \sum_{n=0}^{N} (SET_n - T_{lim}) \times 1_{(SET_n > T_{lim})} \times \Delta t \quad (3)$$

The metric represents the severity of thermal stress over the simulated period, as the sum of all differences between the hour's specific SET ($SETn$) and the fixed comfort limit ($Tlim$) for all hours where $SETn$ is larger than $Tlim$.

Dynamic thermal & energy simulation

Building energy models are developed using the Honeybee plugin from Ladybug Tools (v.1.8.0) within the Grasshopper environment, referencing 3D geometry from Rhino 8 (Robert McNeel & Associates, 2023). Simulations are executed using the EnergyPlus engine via OpenStudio (v.3.7.0), accessed from the plugin (NLR, 2023). The simulation requires hourly weather files, which are generated by converting meteorological data from the National Centers for Environmental Information (NCEI) into EnergyPlus Weather (EPW) format using the Dragonfly plugin from Ladybug Tools (NCEI, n.d.). Data gaps in the hourly sets from the selected weather station at Rotterdam Airport are addressed using interval averaging.

Every parameter in the simulation can introduce uncertainty, affecting the PDE of cooling energy demand (Sun et al., 2016). While parameters such as infiltration and internal gains influence cooling demand, these variables are kept constant to isolate the specific effects of climate variability. The model applies a customized construction set with uniform details (see Section 0), treating walls adjacent to other buildings as adiabatic. Occupancy schedules for mid-rise apartments, natural ventilation setpoints, and infiltration values are defined based on standard presets and retrofit conditions (See Section 0 and Appendix B Table B.2).

For energy quantification, an ideal air-load system is utilized with setpoints of 18°C for heating and 24°C for cooling. Cooling demand is calculated exclusively for the period from May to September. Overheating metrics are evaluated only for living areas and bedrooms, following CIBSE Guide A (2015). Standard Effective Temperatures (SETs) are simulated for non-conditioned states, with the building unit's final representative value determined by the mean of all individual room outputs.

Stage III: cost-benefit analysis

Cost–benefit analysis method

The final stage employs Net Present Value (NPV) as the primary indicator for financial feasibility, consistent with its widespread use in retrofit decision-making literature (Sharbaf & Schneider-Marin, 2025). NPV is calculated by summing the discounted cash flows over the analysis period, with positive values indicating profitability and negative values indicating a failure to achieve cost recovery (Preciado-Pérez & Fotios, 2017). Through uncertainty analysis, this indicator quantifies the risk of non-profitable outcomes and the probability of specific outcome ranges, as is computed as:

$$NPV = \sum_{n=0}^{N} \frac{C_n}{(1+r)^n} \quad (4)$$

where C_n is the net cash flow in year n, r is the discount rate and N is the total number of years.

The analysis period is fixed at 30 years, aligning with common retrofit practices and EU recommendations (Sharbaf & Schneider-Marin, 2025). A discount rate of 3% is utilized to reflect the regional economic context (Groh et al., 2022), following European literature values that typically range between 3% and 4% (Belaïd et al., 2021; Bragolusi & D'Alpaos, 2022; Guardigli et al., 2018; Higney & Gibb, 2024). Settings for cost modelling and other analysis parameters are detailed in Appendix B Table B.1.

Costs are modelled using the global costing method, which aggregates investment, operation, replacement, and maintenance expenditures (Sharbaf & Schneider-Marin, 2025). Investment costs are sourced from national databases, while maintenance and replacement values are estimated based on lifespan ratios from EN15459-1:2017 (*Archidat Bouwkosten*, n.d.; Koninklijk Nederlands Normalisatie-instituut, 2017; RVO, n.d.). Operational costs are defined as variable energy costs calculated using 2024 CBS pricing (CBS, 2025). For heating, fixed costs and tax adjustments are applied where retrofitting involves a transition in energy sources (Wahi et al., 2025).

Sample generation

The cost–benefit analysis is executed through a two-stage digital workflow developed in Python, which first derives a probabilistic representation of energy savings from the simulation results and then evaluates economic outcomes through Monte Carlo simulation (Figure 2). Input data such as pricing, efficiency parameters are retrieved from JSON configuration files, which also reference the simulation results CSV for the selected years. At first, energy values are converted into operational costs using the sourced price assumptions, then these cost datapoints are interpolated into a CDF together with the cumulative probabilities established as per Section 0. Using the CDF, a PDF is constructed as the final probabilistic distribution of operational costs for each scenario.

To determine energy savings, 1000 percentile points are calculated for both the baseline and retrofit scenario distributions. Each retrofit value is subtracted from the baseline to produce 1000 savings values, which inform a new probability estimation utilizing a KDE function. Finally, 10,000 representative savings samples are generated from this distribution to serve as the probabilistic input for the iterative Monte Carlo process.

Risk amalgamation

Risk amalgamation combines parameter uncertainties to evaluate the overall financial feasibility of each retrofit scenario. This second part of the digital workflow uses Monte Carlo simulation to aggregate fixed and variable cost uncertainties, generating 5000 potential NPV outcomes seeking a balance between result stability and computational load. The process employs a Python-based workflow to model cash flows over the 30-year analysis period.

The simulation applies year-dependent discount factors to static costs, including investment, maintenance and replacement. For each iteration, annual energy savings are determined by randomly sampling 30 values from the previously generated set ($n = 10{,}000$). The resulting NPV for each run is calculated by summing the discounted annual costs and savings, and the final records are stored in a CSV format. This process is initially performed for cooling cost assessment, prior to integration into a comprehensive heating and cooling analysis. Supplemental heating-only data are provided in Appendix B.

Financial risk assessment

The NPV results from the Monte Carlo simulation are analysed using descriptive statistics, including the mean, median, standard deviation, and selected percentiles, to outline the range of high-probability outcomes for financial feasibility. This analysis investigates the specific influence of extreme years on CBA results by assessing the relationship between sampled savings and the resulting NPV. While a multi-year analysis assumes an average recurrence rate for annual extremes, the risk of significantly exceeding this frequency represents a 'worst-case' scenario. To identify such scenarios, a binomial test is applied to calculate the minimum number of extreme years required for the cumulative probability of occurrence to fall near a 5% significance level ('Binomial Test', 2008). Since the analysis evaluates time in discrete years, achieving an exact 5% target can be met by the closest practical approximation. Simulation runs meeting this criterion are isolated to determine worst-case NPVs, representing financial performance under exceptionally adverse climatic conditions.

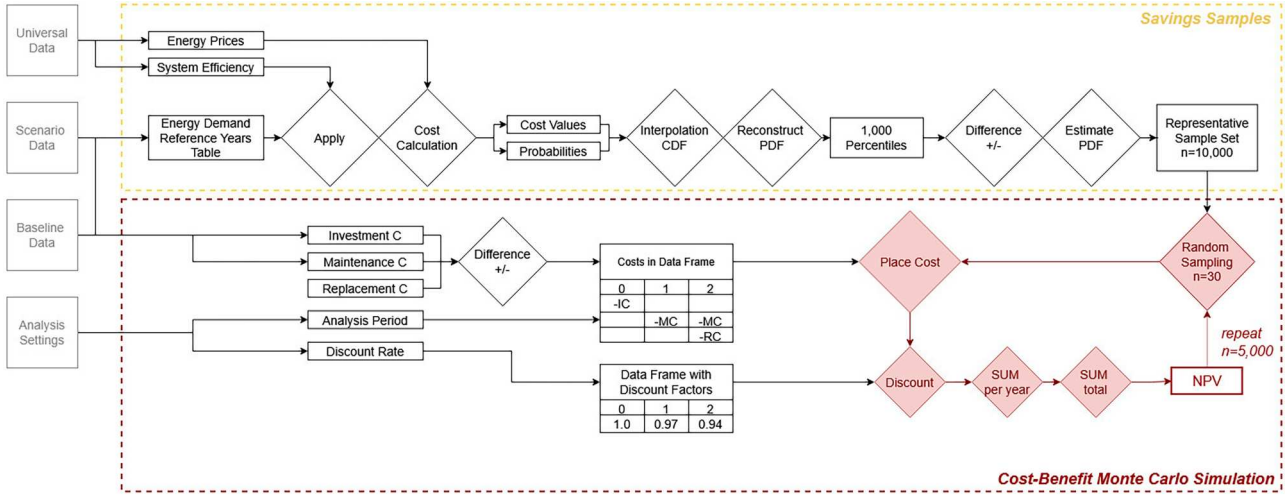


Figure 2. Python script workflow for cost-benefit analysis with Monte Carlo simulation.

Case study specification

The case study building is located in the Bospolder-Tussendijken district of Rotterdam West, an area undergoing a municipally led heat transition (2022–2026) (Gemeente Rotterdam, 2021). The analysed unit belongs to a multi-family 1952 porch-house row, a typical Dutch residential typology comprising eight apartments across four storeys (RVO, 2020). The neighbourhood is characterized by low housing quality and high energy demand, resulting in socio-technical vulnerability to energy poverty and heat-related risks (Gemeente Rotterdam, 2024). The building therefore constitutes a representative testbed for resilience-oriented retrofit strategies.

Architectural and structural data were obtained from archival drawings and municipal consultations (Stadsarchief Rotterdam, n.d.). The baseline scenario represents the pre-retrofit condition, featuring non-insulated solid brick masonry, single glazing and gas-condensing boilers for each residential unit. To translate heat resilience benefits into energy savings within the CBA and ensure a coherent performance benchmark, active cooling is assumed for this baseline. Wall-system and opening specifications were standardized in the energy model. Calibration was performed using an average heating demand of 205.33 kWh/m², derived from 15 existing energy labels within the housing row (Rijksoverheid, n.d.). Table 1 summarizes the case study specifications.

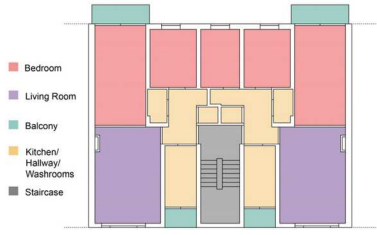
Retrofit scenario development

Retrofit scenarios were evaluated against the baseline, assuming an air-conditioning system with a conservative Coefficient of Performance (COP) of 2.9 in all cases. The primary objectives were to improve energy efficiency and reduce overheating, benchmarked using the KPIs defined in Section 0. As a secondary objective, heating efficiency was also assessed to examine the integration of overheating mitigation within standard retrofit practice.

Retrofitting options were assessed across energy supply systems, envelope components (walls, openings, floors, and roofs), and energy sources. Measures were evaluated by mitigation potential, cost, and intervention depth, categorized as simple (S), medium (M) and deep (D). Thermal resilience measures target solar gains via textile awnings and high-albedo paint on the south-western façade, while heating upgrades include switching to district heating, double-glazing and exterior insulation, in alignment with the EU TABULA study and Dutch regulations (RVO, 2020; TABULA WebTool, 2014). In total, five distinct scenarios were developed: (i) three 'Simple' variations, testing passive cooling measures alongside district heating, (ii) a 'Medium' scenario incorporating window retrofit and shading, and (iii) a 'Deep' scenario integrating all measures, including full façade insulation (Table 2).

Table 1. Case study building specifications.

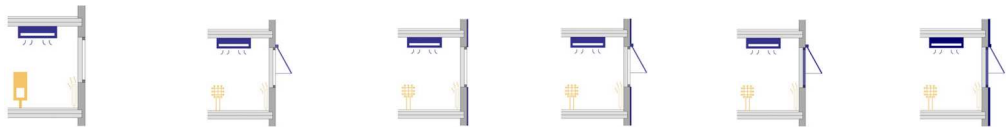




Case study building	
Location	Tussendijken, Rotterdam
Typology	Porched House
Construction year	1952
Number of stories	4 stories; highest floor +9.90 m
Number of apartments	8 apartments per unit
Total floor area	505.33 m^2 per unit
Window to wall ratio	~32%
Heating system	Individual gas condensing boilers ($\eta = 0.85$)
Annual heating demand average	205,33 [kWh/m^2]
Exterior wall-system	Solid brick masonry (23 cm; 1.83 [W/m^2K])
Interior wall-system	Drywall-system 12 cm: 0.62 W/(m^2K)
Interior floors	*Assumption:* concrete floor slab (100 mm: 1.16 [W/(m^2K)])
Openings & Windows	Single glazing (5.2 [W/m^2K])
Infiltration	*Assumption:* leaky (0.0006 [m^3/s per m^2])

*The assumptions are based on typical values provided by the software material and construction library.

Table 2. Retrofit scenario specifications.



Scenario	*Baseline*	*S01-Simple Shading*	*S02- Simple Paint*	*S03-Simple Combi*	*M01-Medium shading*	*D01-Deep Shading-paint*
Cooling system	**Air-conditioning (COP: 2.9)**	Air-conditioning	Air-conditioning	Air-conditioning	Air-conditioning	Air-conditioning
Heating system	Gas-boiler ($\eta = 0{,}85$)	**District heating (η = 1,0)**	District heating	District heating	District heating	District heating
Wall transmission	1.83 W/(m^{2}K)	1.83 W/(m^{2}K)	1.83 W/(m^{2}K)	1.83 W/(m^{2}K)	1.83 W/(m^{2}K)	**0.22 W/(m^{2}K)**
Window transmission	5. W/m^{2}K	5.2 W/m^{2}K	5.2 W/m^{2}K	5.2 W/m^{2}K	**1.65 W/m^{2}K**	1.65 W/m^{2}K
Infiltration	0.0006 [m^3/s per m^2]	0.0006 [m^3/s per m^2]	0.0006 [m^3/s per m^2]	0.0006 [m^3/s per m^2]	**0.0003 [m^3/s per m^2]**	**0.0001 [m^3/s per m^2]**
Façade Albedo/ Absorption	0.65	0.65	**0.2**	0.2	0.65	**0.2**
Sol.& Vis. reflectance of shading	/	**0.1**	/	0.1	0.1	0.1

Results

Stage I: climate data analysis

Applying the heatwave definition (Section 0) to the 30-year dataset, 11 heat hazards were identified (Figure 3). These events occurred exclusively in July and August, with durations ranging from 6 to 20 days and a mean of 10.5 days. The longest periods were recorded in 2018 (20 days) and 2006 (16 days). 2019 was unique in featuring two distinct events separated by a 28-day interval.

To distinguish acute thermal stress during heatwaves from annual cumulative heat exposure, annual degree-days above 25°C were compared with heatwave-specific values (Figure 4). Years without a designated heat wave are represented with a hazard value of zero. Hazard intensities ranged from 22.4 to 77.5 degree-days. The years with the highest values, 2018, 2006, 2020 and 2019, correspond to those with the longest total heat-wave duration, yet their degree-day values are significantly higher than those of other heatwave years.

Annual values exhibited significant dispersion, from 13.9 degree days in 2007 to 133.0 degree days in 2006. The highest annual values were dominated by the top six heatwave years. However, the specific intensity within this group varied considerably. For instance, 2006 reached the annual maximum of 133.0 but ranked second in hazard intensity at 69.5. Conversely, 2018 recorded the maximum hazard intensity of 77.5 while ranking second annually at 127.0. Notably, 1995 and

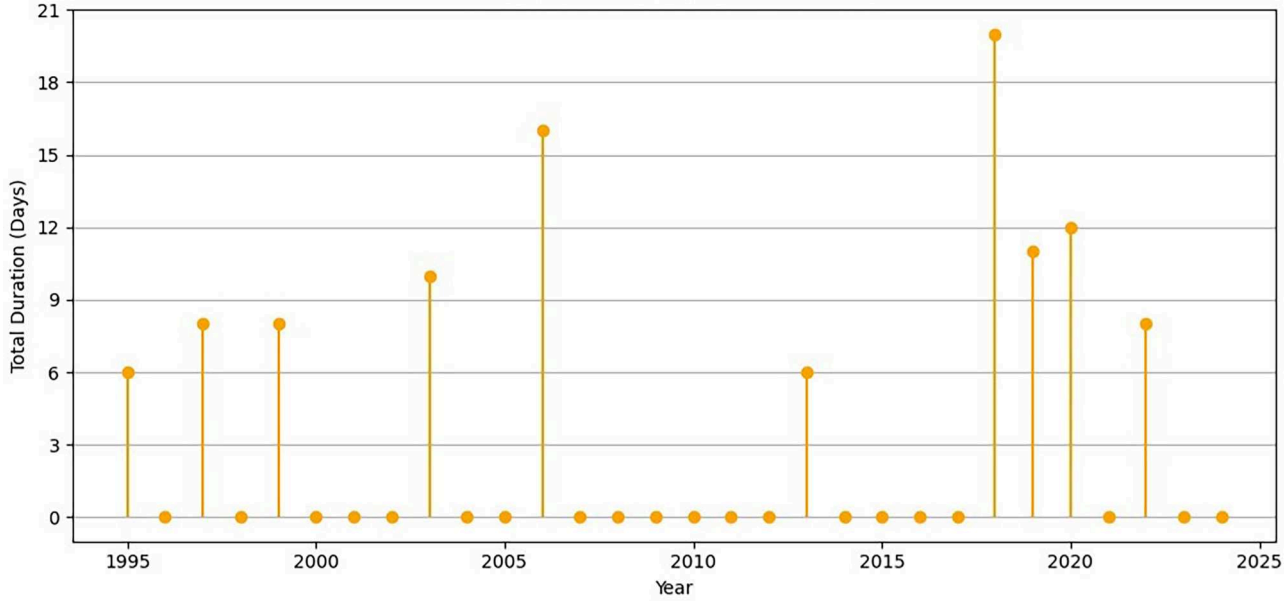


Figure 3. Detected heatwaves and their duration for the period 1995–2024.

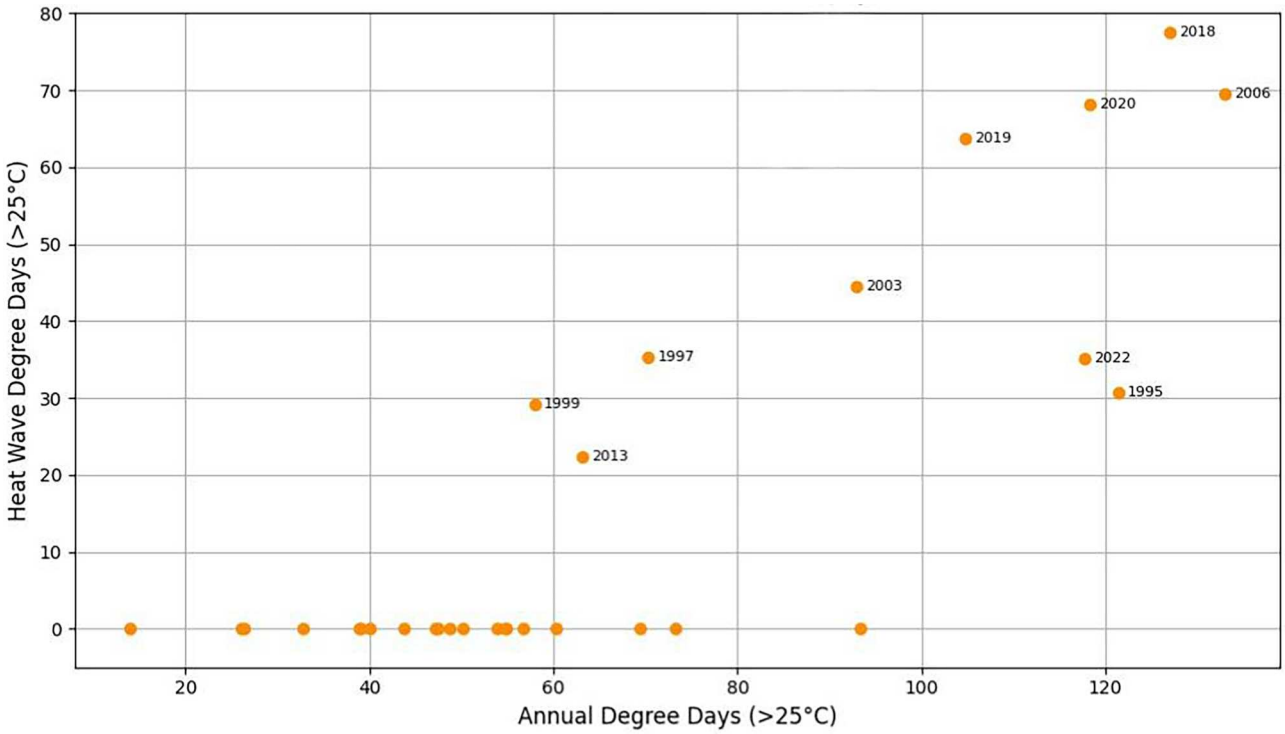


Figure 4. Temperature intensity of warm days (>25°C) annual vs. heatwave period with heatwave years labelled.

2022 featured high annual loads but heatwave intensities comparable to less severe heat years.

Subsequent impact estimation quantified the relevance of heatwave periods within these high-stress years. Dynamic simulations of the six years with the highest thermal stress were conducted to determine baseline cooling energy demand and overheating metrics (Table 3). These assessments treated annual and heatwave periods separately, with the latter incorporating an eight-day buffer before and after each event. Heatwave periods contributed between 42.8% and 80.4% of the total annual cooling energy demand. Regarding thermal comfort, hazards accounted for 31.1% to 77.8% of annual overheated hours and 11.5% to 85.5% of overheated degree hours. The proportional contribution to energy demand was more substantial, consistently representing at least 42% of the annual total.

Transitioning from meteorological metrics (hazard analysis) to building impact revealed a divergence in the ranking of extreme years. Although 2006 and 2018 dominated the degree-day analysis, 2020 proved most severe for building performance. It recorded the highest annual cooling demand of 17,515 kWh alongside the greatest overheating duration. The ranking of cooling demand, comprising 2020, 2006, 1995 and 2018, demonstrates that ambient heat intensity does not linearly translate into the building's internal thermal response.

Annual extreme definition

While hazard analysis highlights the contribution of heatwave periods to thermal stress, a probabilistic assessment was conducted to quantify the risk of performance variability driven by extremes. A CDF for cooling demand was modelled using the 30-year baseline simulation to contextualize reference years within the probabilistic distribution (Figure 5). Consistent with the degree-day analysis, the six years with the highest annual intensity recorded the greatest cooling demands. However, the presence of a heatwave did

Table 3. Annual vs. heatwave impact for the baseline scenario.

Year	Annual cooling demand [kWh]	Heatwave cooling demand ±8 days [kWh]	Annual overheated hours [h]	Heatwave overheated hours ±8 days [h]	Annual overheated degree hours [dh]	Heatwave overheated degree hours ±8 days [dh]
1995	16,510.48	7073.5	151.0	47	365.0	42.0
2006	17,077.96	9921.56	117.0	84	117.0	100.0
2018	15,263.55	10,556.96	113.0	69	553.0	126.0
2019	14,697.04	6518.48	101.0	59	191.0	152.0
2020	17,515.24	14,076.65	162.0	126	309.0	189.6
2022	14,071.11	6660.91	174.0	65	588.0	233.0

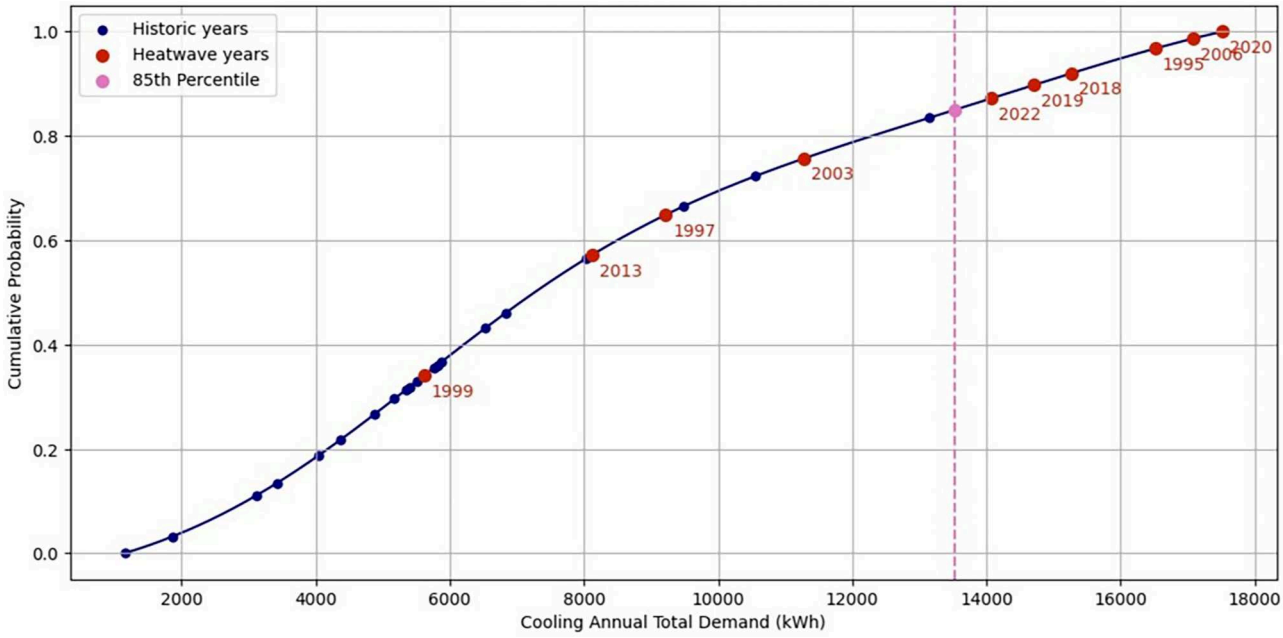


Figure 5. Cumulative Distribution Function of annual cooling energy demand. The plot distinguishes between standard historic years (blue) and years featuring heat hazards (red). The clustering of heatwave years above the 85th percentile illustrates the connection between heat hazards and increased cooling loads.

not necessarily result in an exceptional annual total. Years with moderate hazards, such as 1999 and 2013, were distributed across standard demand ranges with cumulative probabilities between 34.06% and 75.72% (Table 4).

A robust 'annual extreme' threshold was established at the 85th percentile, equating to 13,524.66 kWh. This value was determined by the clustering of the top six extreme years and includes a marginal surcharge on the 2022 data point. Statistically, this threshold implies a 15% annual probability of an extreme cooling event. Although the expected frequency over a 30-year period is 4.5 years, the historical dataset recorded six occurrences. This indicates a higher incidence of high-demand events than predicted by standard probability density estimation.

Table 4. Annual cooling demand and corresponding cumulative probability of heatwave years.

Heatwave years	Cooling demand annual total [kWh]	Estimated cumulative probability [%]
1999	5614.74	34.06%
2013	8124.78	57.23%
1997	9212.36	64.86%
2003	11,284.98	75.72%
2022	14,071.11	87.21%
2019	14,697.04	89.74%
2018	15,263.55	92.01%
1995	16,510.48	96.74%
2006	17,077.96	98.66%
2020	17,515.24	100.0%

The year 2020 recorded the maximum cooling demand, aligning with its identification as the most impactful heatwave regarding duration and intensity. This year was selected as the representative 'annual extreme' for subsequent cross-domain performance comparisons, serving as the benchmark for quantifying overheating indicators under maximum energy load conditions.

Stage II: energy simulation

For the probability estimation, the seven reference years for cooling demand were determined using the method described in Section 0. At first, the percentile values for the 5th, 25th, 50th, 75th and 95th percentiles were calculated, and the closest match in actual annual values was identified (Table 5). Then, the actual percentile value on the CDF was estimated for the real years, e.g. the 5th percentile reference year 2021 corresponding to 3% cumulative probability (Table 5). The deviation between the identified vs actual percentile in terms of cumulative probability is only 1–2%. Additionally, the minimum and maximum extreme years, 2007 and 2020, were added to complete the reference set.

Results on cooling energy performance

Figure 6 illustrates the distribution of Cooling Energy Use Intensity (Cooling EUI) across the retrofit scenarios. The plot denotes the mean, median, 85th

Table 5. Annual cooling demand percentiles and closest matching reference year.

Percentile	~ Total annual demand [kWh]	Closest matching year	Total annual demand [kWh]	Corresponding actual percentile [%]
Minimum (0)	1160.01	2007	1160.01	0
5	2178.51	2021	1862.97	3
25	4697.22	2017	4868.62	27
50	7250.99	2001	6832.23	46
75	11,119.54	2003	11,284.98	76
95	16,032.66	1995	16,510.71	97
Maximum (100)	17,515.24	2020	17,515.24	100

percentile, and the 2020 year (maximum value). Cooling energy efficiency improved across all retrofit scenarios. The baseline mean Cooling EUI of 5.99 kWh/m² fell to 5.62 kWh/m² with shading (S01) and 5.76 kWh/m² with high-albedo paint (S02). Combined measures (S03) achieved a further reduction to 5.42 kWh/m². The Medium scenario (M01) yielded a mean similar to S01 at 5.57 kWh/m², while the Deep scenario (D01) performed comparably to S03 at 5.45 kWh/m².

Under extreme conditions, baseline energy intensity increased significantly to 9.05 kWh/m² at the 85th percentile and 11.95 kWh/m² during the 2020 year. The Deep scenario (D01) was most effective at mitigating these peaks, limiting intensity to 8.40 and 11.23 kWh/m², respectively. The S03 retrofit followed closely with values of 8.45 and 11.36 kWh/m². Table 6 details percentage improvements relative to the baseline. Relative effectiveness diminished during extreme events across all scenarios. In S01, the improvement decreased from 6.2% at the mean to 4.8% at the 85th percentile and 3.2% at the 2020 maximum. This consistent trend indicates reduced efficacy during peak thermal loads.

Results on heat resilience

The heat resilience of retrofit scenarios was evaluated using OH and ODH above the 28°C SET limit for the extreme year 2020 (Figure 7). The baseline recorded 162 OH and 309 ODH. Simple shading (S01) reduced overheating duration by 21% and intensity by 37%. Simple paint (S02) yielded lower reductions of 16% and 23%. Among simple interventions, the combined scenario (S03) was the most effective for duration, achieving a 35% improvement and reducing intensity by 53%. The Medium (M01) scenario performed similarly to S02. However, the Deep (D01) retrofit demonstrated the highest resilience, achieving the greatest intensity reduction of 59% to a low of 128 ODH.

Direct comparison between maximum Cooling EUI and heat resilience indicators for the year 2020 reveals

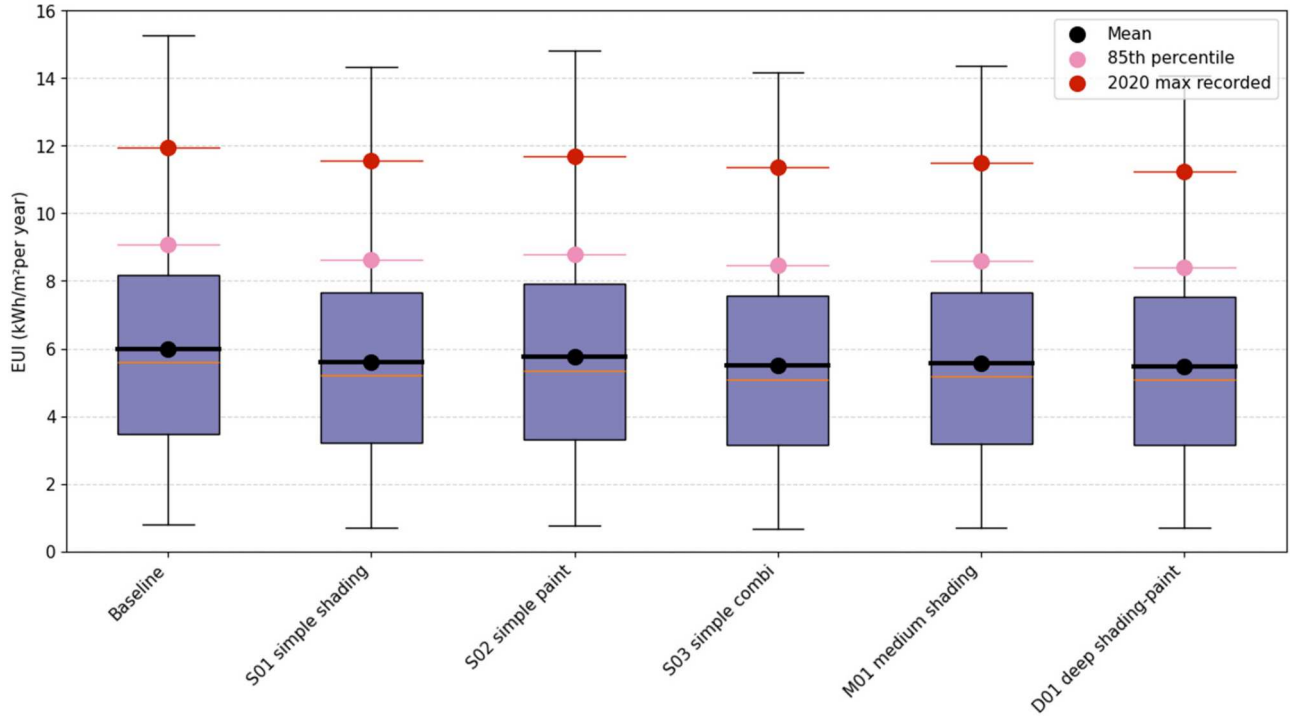


Figure 6. Boxplots of cooling energy use intensity (EUI) for the baseline and retrofit scenarios. The boxplots summarize the distribution of simulated outcomes: the box represents the interquartile range (25th–75th percentiles), the horizontal line inside the box indicates the median, and the whiskers show the range of typical values. The mean value and the 85th percentile are explicitly labelled for each scenario, together with the 2020 reference value for comparison.

Table 6. Building Performance Results for retrofitting scenarios: energy use intensity as mean value, 85th percentile and maximum value (2020 year), overheated hours and overheated degree hours for 2020 year.

Scenario	Cooling EUI mean	Δ Difference to baseline [%]	Cooling EUI 85th percentile	Δ difference to baseline [%]	Cooling EUI 2020 max	Cooling EUI 2020 max Δ [%]	Overheated hours (2020) > 28 SET	Δ difference to baseline [%]	Overheated degree hours (2020) > 28 SET	Δ difference to baseline [%]
Baseline	**5.99 kWh/m²**	/	**9.05 kWh/m²**	/	**11.95 kWh/m²**	/	**162 h**	/	**309 dh**	/
S01 shading	5.62 kWh/m²	−6.2%	8.62 kWh/m²	−4.8%	11.57 kWh/m²	−3.2%	128 h	−21%	193 dh	−37%
S02 paint	5.76 kWh/m²	−3.8%	8.79 kWh/m²	−2.9%	11.71 kWh/m²	−2.0%	136 h	−16%	237 dh	−23%
S03 combi	5.42 kWh/m²	−9.5%	8.45 kWh/m²	−6.6%	11.36 kWh/m²	−4.9%	105 h	−35%	145 dh	−53%
M01 shading	5.57 kWh/m²	−7.0%	8.57 kWh/m²	−5.3%	11.49 kWh/m²	−3.8%	137 h	−15%	235 dh	−24%
D01 shading-paint	5.45 kWh/m²	−7.5%	8.40 kWh/m²	−7.2%	11.23 kWh/m²	−6.0%	107 h	−34%	128 dh	−59%

a clear mismatch in performance. While retrofit scenarios delivered thermal resilience benefits, the corresponding reductions in maximum Cooling EUI were marginal and ranged only between 2.0% and 6.0%. The relative effectiveness of these measures on thermal discomfort was up to 11 times greater than the energy efficiency improvements. For instance, the S01 reduction in overheating duration was 6.5 times higher than the Cooling EUI reduction of 3.2% (Table 6). This condition was more pronounced for intensity, where the reduction in degree hours was 11.6 times greater than the energy improvement. Similarly, the S03 scenario achieved a 10.8 times larger reduction in overheating intensity compared to peak energy demand.

Stage III: cost-benefit analysis

Energy cost savings were calculated for each scenario, and their probabilistic distributions were derived according to the established methodology (Section 0) (Figure 8). This analysis verified that the previously defined 85th-percentile threshold for energy use remains a valid benchmark for monetary savings within the CBA.

While costs scale linearly with demand, savings exhibit non-linear behaviour across the extreme hazard range. Table 7 indicates that savings tend to saturate or reverse at the highest energy use levels. For most retrofit scenarios, peak savings occur between the 85th and 100th percentiles of energy use. Consequently, savings for the 2020 maximum demand were lower than those at the 85th percentile. Specifically, savings in S01, S02, and S03 decreased by 11%, 1.9%, and 6.7%, respectively, at maximum energy use. Similarly, Medium (M01) savings for 2020 were 4.3% lower than the €59.9 recorded at the 85th percentile. Only the Deep scenario (D01) saw 2020 savings exceeding the 85th percentile by 5.7%.

This non-linear relationship makes the 85th percentile insufficient as the sole threshold for cost–benefit analysis, as it excludes the lower savings in peak-demand years. To establish a more representative range, the cumulative probabilities of the savings variable matching the minimal savings in the extreme energy-use range were identified. S01 required a 65.9% probability to capture its €47.5 minimum, while S03, S02, and M01 required 73.1%, 80.2%, and 77.7%, respectively. For D01, the threshold remained at 85.0%.

A uniform threshold was therefore selected at the 65th percentile to ensure cross-scenario comparability. This value was chosen as the closest practical threshold to the 65.9% probability required to capture the 2020 year for S01. While ensuring coverage for S01, this uniform threshold introduces minor savings divergences in

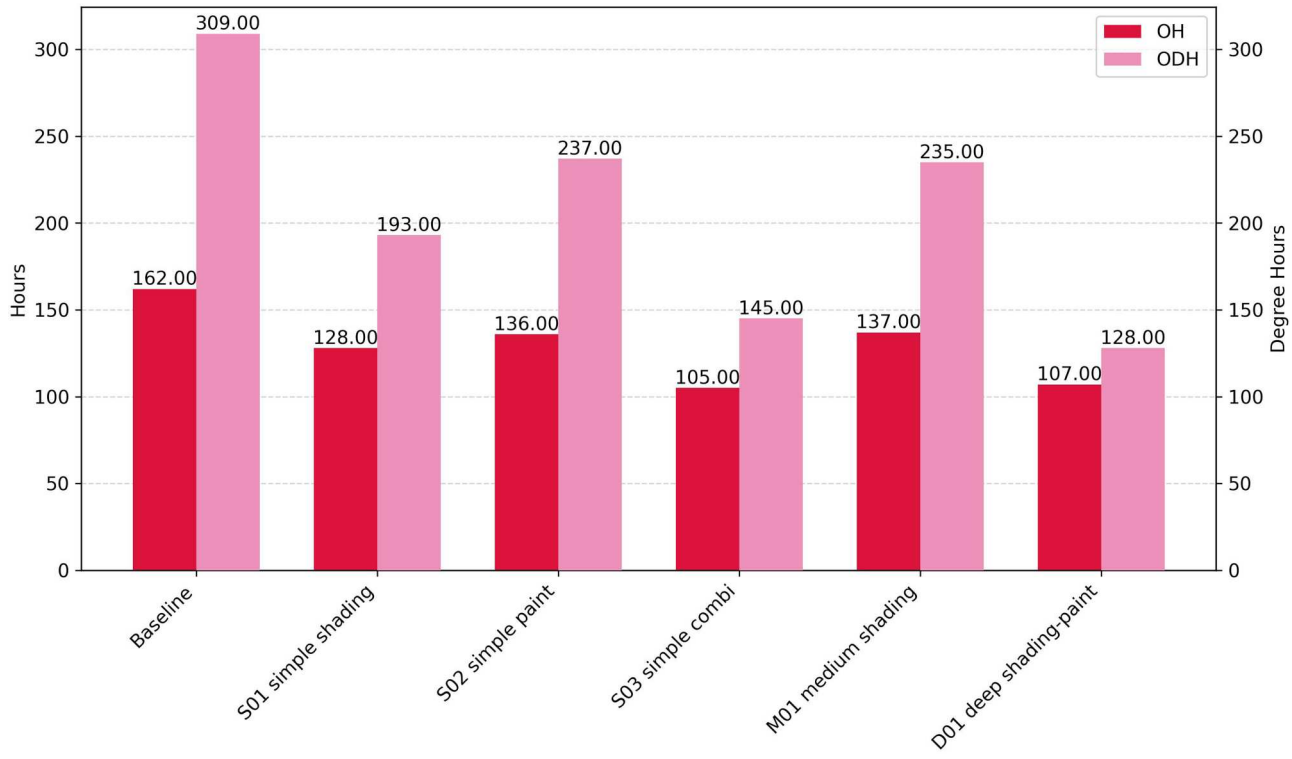


Figure 7. Heat resilience indicator bar chart for baseline and retrofit scenarios incl. overheated hours and overheated degree hours referencing 2020.

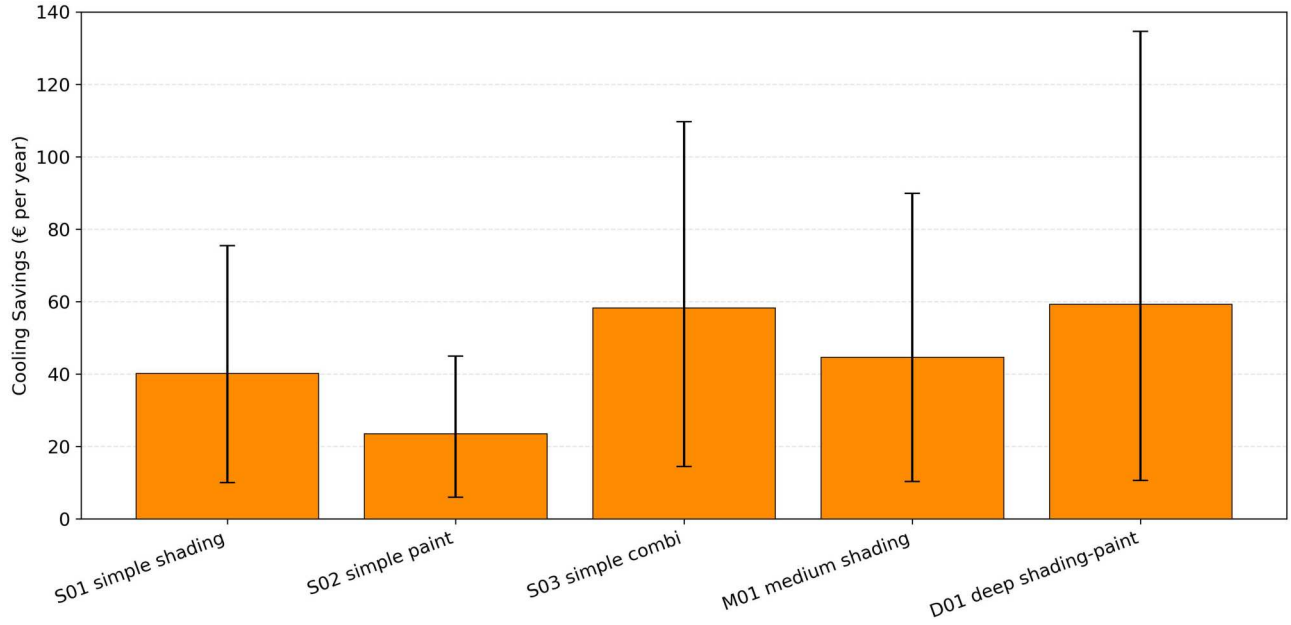


Figure 8. Bar chart of cooling energy savings for retrofit scenarios.

S02, S03 and M01 (€2.50–€5.40) and a €15.50 deviation for D01. The adjusted threshold includes the top 35% of years and captures increased energy demand values that are not exclusively restricted to identified heat hazards.

Based on this selection, the 65th-percentile threshold defines the 'worst-case' multi-year scenario in the CBA. Statistically, the expected recurrence over 30 years is 10.5 years. A binomial test indicates that a frequency of 15 or more years above this threshold corresponds to a cumulative probability of 6.52%, which falls near the standard 5% significance level. Consequently, any Monte Carlo iteration with 15 or more years above

Table 7. Energy use and cost savings at cumulative probability (CP) 65%, 85% and 100%.

Scenario	65% CP energy use [kWh]	85% CP energy use [kWh]	100% CP (2020 year) energy use [kWh]	% CP of minimal savings in extreme energy use range	Energy use at % CP savings [kWh]	Savings [€] at 65% CP	Savings [€] at 85% CP	Savings [€] at 100% CP (2020 year)
Baseline	3421	4586	6040	/	/	/	/	/
S01 – simple shading	3226	4366	5844	65.9%	3275	€ 47.3	€ 53.4	€ 47.5
S02 – simple paint	3307	4459	5915	80.2%	4122	€ 27.8	€ 30.9	€ 30.3
S03 – simple combi	3137	4265	5741	73.1%	3562	€ 68.9	€ 77.9	€ 72.7
M01 – medium shading	3207	4339	5804	77.7%	3876	€ 51.9	€ 59.9	€ 57.3
D01 – deep shading-paint	3142	4244	5678	85.0%	4244	€ 67.7	€ 83.2	€ 88.0

the 65th-percentile savings threshold was classified as a worst-case scenario.

Cooling cost analysis

The cost recovery potential for simple passive cooling strategies (S01–S03) was initially assessed through a cooling-cost-only CBA. For the Medium (M01) and Deep (D01) renovation scenarios, such analysis was deemed methodologically inconsistent, as measures primarily target heating efficiency. NPV distributions were generated via 5000 Monte Carlo iterations, with main statistical properties summarized in Table 8. All scenarios yielded negative mean NPVs: €−9031 for S01, €−9376 for S02, and €−18,513 for the combined S03 scenario, indicating that costs are high relative to expected savings. Standard deviations remained below €100, though dispersion increased in scenarios with higher potential savings.

Worst-case outcomes, representing iterations where high-demand years occur with exceptional frequency, were identified using the 65th percentile savings threshold and a 15-year recurrence rate, as discussed above. These outcomes are concentrated at the highest values in the NPV distribution (Figure 9). The frequency of worst-case results within the total population was 4.74% for S01, 3.92% for S02, and 3.84% for S03. For S01, the worst-case NPV ranged from €−9052 to €−8870. S02 and S03 ranges were €−9378 to €−9285 and €−18,533 to €−18,233, respectively (Table 8).

Comparison with the 99th percentile of the total population reveals that all maximum worst-case results exceeded the 99th percentile threshold by up to €100. Average NPVs for iterations with exactly 15 extreme samples were €−8963 (S01), €−9332 (S02), and €−18,404 (S03). Overall, worst-case conditions improved the mean NPV by €72–€114 for S01, €45–€67 for S02, and €108–€168 for S03, indicating that extreme heat marginally enhances the economic performance of retrofit measures, despite NPVs remaining negative.

A parametric sensitivity test was conducted for the cooling cost analysis on the variables assumed constant as the discount rate, electricity price and air-conditioning system efficiency (COP) to quantify their influence on the financial outcome. Mean annual energy demand was held constant to isolate the effects of economic and system-efficiency assumptions (Table 9). Across the simple scenarios (S01–S03), increasing electricity prices and discount rates consistently improved the NPV. Conversely, increasing the COP exhibited an inverse relationship and reduced overall returns. The magnitude of influence varied by

Table 8. NPV results for retrofit scenarios accounting for cooling cost savings.

Scenario	S01 shading	S02 paint	S03 combi
NPV Mean [€]	−9031.41	−9376.06	−18512.92
Standard deviation [€]	50.22	28.84	74.71
% of negative values	100.00%	100.00%	100.00%
Number of worst-cases (incl. ≥ 15 extreme savings)	237	196	192
Percentage of worst-cases (incl. ≥ 15 extreme savings)	4.74%	3.92%	3.84%
Minimum value for worst-case [€]	−9052.59	−9378.66	−18533.23
Maximum value for worst-case [€]	−8870.19	−9285.63	−18233.11
Average worst-case (incl. = 15 extreme savings) [€]	−8962.70	−9332.37	−18403.98
99th Percentile [€]	−8917.86	−9309.54	−18344.36

scenario. Variations in the discount rate (0–6%) caused the greatest deviation in the combined scenario (S03) at approximately €3944, while the impact in S01 and S02 ranged between €747 and €2437. Electricity price fluctuations produced deviations between €493 and €1354. Finally, system efficiency shifted the NPV by €563 in S02 and €1549 in S03. The sensitivity testing resulted in a range of outcomes all exhibiting negative NPVs, further proving that the retrofits are not financially viable.

Integrated analysis: heating and cooling cost

The cooling-only assessment was extended to integrate heating performance, providing a comprehensive energy and financial overview. The results are described through the mean, standard deviation and percentiles (Table 10). The separate analysis on heating energy performance and CBA is provided in Appendix B (Table B.4). The integration of cooling and heating costs significantly shifts the financial outlook. Only simple shading (S01) and the deep retrofit (D01) yielded positive mean NPV, meaning that, on average, these scenarios generated financial gains. The D01 scenario demonstrated the most robust performance with 100% positive outcomes ranging from €14,346 to €20,573. Although S01 achieved a positive mean NPV of €490, it carried a 12.12% probability of failing to recover costs. Remaining scenarios recorded negative results, with S03 yielding the lowest mean at €−18,274.

Financial risk dispersion varied significantly, with standard deviations ranging from €210 (S02) to €1335 (D01). Intensive interventions (M01 and D01) exhibited much wider dispersion than simple scenarios. Notably, worst-case climate conditions showed no specific clustering at the distribution extremes. For S01, worst-case NPVs spanned from €−631.50 to €1574.75, compared to the 1st and 99th percentiles of €−486.19 and €1481.36, respectively. The mean NPV for runs with exactly 15 extremes in S01 was €490.37, almost identical to the overall mean of €490.20. Consequently, no distinct NPV range specifically relates to worst-case conditions in the integrated analysis.

To evaluate the underlying drivers of these results, the specific impact of heating vs cooling savings on the NPV was compared. Strong positive correlations were observed for heating savings across all scenarios, with R^2 values ranging from 0.842 to 0.934 (Figure 10(a)). Conversely, cooling savings showed negligible influence on NPV outcomes (Figure 10(b)). The lack of a clear trend reflects both their small magnitude relative to heating savings (approximately 30 times lower) and the high variability across scenarios and extreme years.

Discussion

The proposed probabilistic framework explicitly links heat extremes with building performance (energy efficiency and thermal comfort) and their monetary implications. Unlike conventional retrofit CBAs, which typically rely on deterministic climate assumptions and energy-focused assessments (S. Sharbaf & Schneider-Marin, 2025; Sun et al., 2016), this approach uses Monte Carlo simulation to propagate climate uncertainty into financial risk metrics. It therefore provides a methodological basis for integrating heat resilience considerations into long-term retrofit investment assessment. By moving beyond a single, static design scenario to define 'annual extremes' through an 85th percentile threshold, the framework evaluates a realistic spectrum of recurring extreme heat events (Machard et al., 2024). This demonstrates how climate uncertainty can be systematically translated into quantifiable hazard inputs for retrofit assessment.

Application of the framework revealed a pronounced disparity between thermal comfort and energy performance. For the analysed Dutch building, shading combined with high-albedo paint (S03) reduced overheating intensity by 53% during annual extremes, whereas cooling energy demand decreased by only 2.0–6.0%. Sensitivity analysis further showed that improvements in cooling system efficiency (COP) reduced the operational value of passive measures by satisfying cooling demand more efficiently. Together,

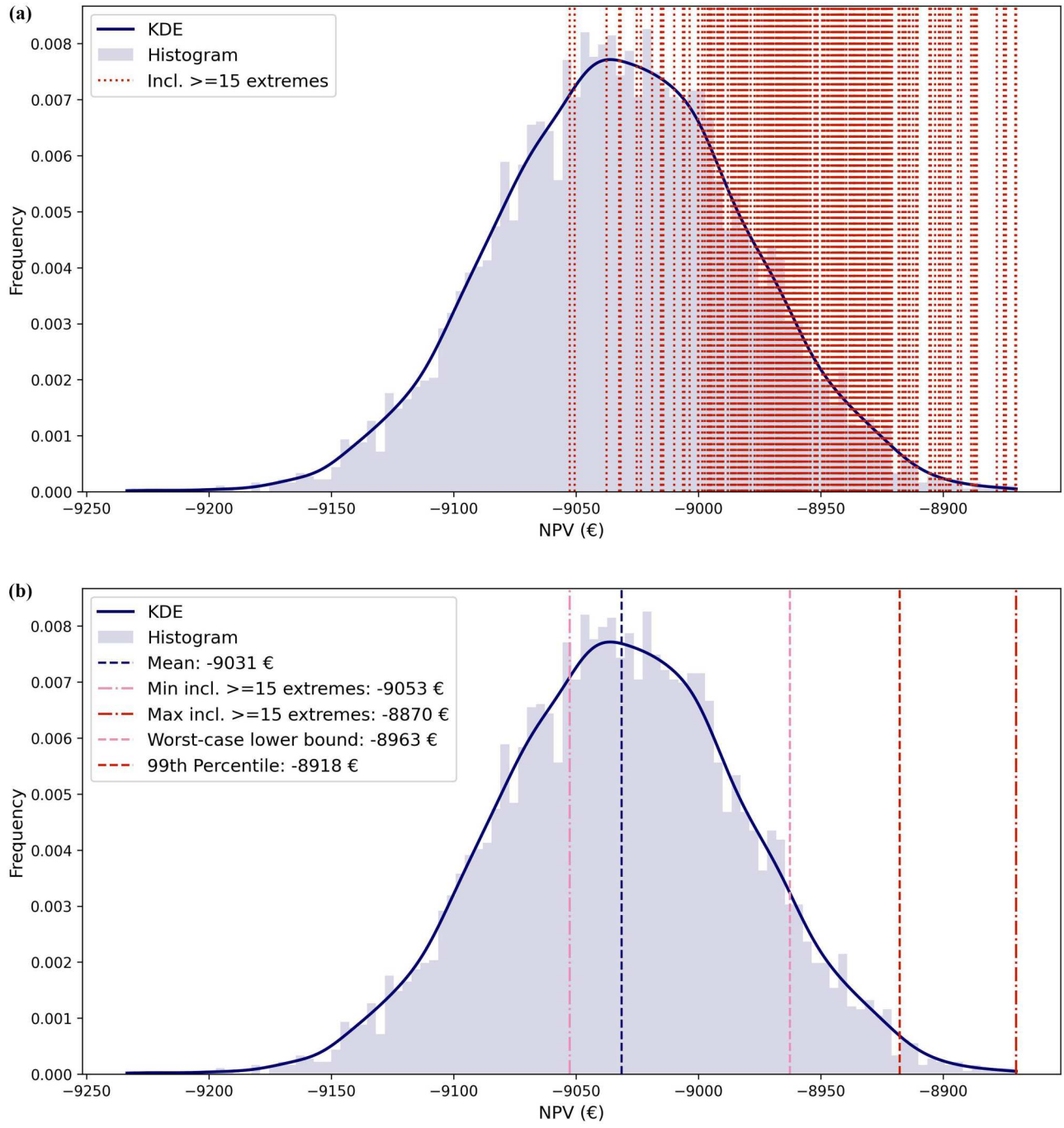


Figure 9. NPV Distribution for S01 Simple shading (only cooling cost); identifying where the critical savings value (65th percentile) was surpassed at least 15 times (a) Full NPV distribution from the Monte Carlo simulation. Red dotted lines indicate simulation runs in which extreme cooling years (above the 65th percentile savings threshold) occur at least 15 times within the 30-year period; (b) Range of financial outcomes under these worst-case climatic conditions, showing the minimum and maximum NPVs among the identified runs. The pink marker indicates the mean NPV for the ≥15 extreme-year cases relative to the 99th percentile of the overall NPV distribution.

these results demonstrate that, for this temperate climate case, cooling energy savings are not an adequate proxy for the resilience benefits of passive retrofit measures. A framework that evaluates only operational energy could substantially underestimate improvements in thermal resilience. This finding highlights the importance of assessing retrofit strategies across multiple performance domains, capturing avoided heat stress and health co-benefits rather than relying solely on energy-based metrics, consistent with several recent studies (Brogno et al., 2025; Krelling et al., 2024; Lee et al., 2024; Sheng et al., 2023).

Table 9. Parameter sensitivity test for varying discount rate, electricity price, COP air-conditioning.

Parameters	–	–	–	reference	+	++	+++
Discount rate	0%	1%	2%	3%	4%	5%	6%
NPV S01	−9604.41	−9420.72	−9267.06	−9137.9	−9028.82	−8936.24	−8857.3
NPV S02	−10652.53	−10006.24	−9451.86	−9451.86	−8975.88	−8566.84	−8215.0
NPV S03	−21020.69	−20081.64	−19280.65	−18596.25	−18010.48	−17508.28	−17076.99
Electricity price	0.093	0.143	0.193	0.243 Euro/kWh	0.293	0.343	0.393
NPV S01	−9572.24	−9427.46	−9282.68	−9137.9	−8993.12	−8848.34	−8703.56
NPV S02	−9698.35	−9616.18	−9534.02	−9451.86	−9369.69	−9287.53	−9205.37
NPV S03	−19273.07	−19047.47	−18821.86	−18596.25	−18370.65	−18145.04	−17919.44
COP Air-conditioning	1.4	1.9	2.4	2.9	3.4	3.9	4.4
NPV S01	−8384.02	−8767.57	−8991.31	−9137.9	−9241.38	−9318.32	−9377.77
NPV S02	−9024.02	−9241.69	−9368.67	−9451.86	−9510.58	−9554.25	−9587.99
NPV S03	−17421.49	−18019.18	−18367.83	−18596.25	−18757.5	−18877.39	−18970.04

Table 10. NPV results for retrofit scenarios, including heating and cooling cost savings; further outlining worst-case condition results.

Scenario	S01 shading	S02 paint	S03 combi	M01 shading	D01 shading-paint
NPV Mean [€]	490.20	−9163.11	−18274.74	−11652.29	17461.66
Standard Deviation [€]	423.61	210.30	232.76	749.69	1335.65
Confidence interval 95% [€]	−332.35–1340.75	−9555.51 to −8735.34	−18721.41 to −17802.89	−13105.84 to −10155.79	14884.07–20048.46
1st percentile NPV [€]	−486.19	−9630.57	−18792.69	−13346.34	14346.67
99th Percentile NPV [€]	1481.36	−8655.72	−17718.22	−9931.61	20573.86
Negative results [%]	12.12%	100.00%	100.00%	100.00%	0.00%
Number of worst-cases (incl. ≥ 15 extreme savings)	246	169	208	411	538
Percentage of worst-cases (incl. ≥ 15 extreme savings) [%]	4.92%	3.38%	4.16%	8.22%	10.76%
Minimum value for worst-case [€]	−631.5	−9611.55	−18755.74	−14601.37	14263.56
Maximum value for worst-case [€]	1574.75	−8526.28	−17406.66	−9668.29	21244.29
Average worst-case (incl. = 15 extreme savings) [€]	490.37	−9083.61	−18175.15	−11620.43	17583.60

Comparison of retrofit strategies further illustrated the framework's ability to distinguish performance across intervention levels. For the analysed case study, combined passive measures consistently produced the largest reductions in overheating among low-intervention options, aligning with recent literature identifying combined approaches as the most robust against overheating (Le et al., 2025; Zhang et al., 2021). In this case, shading (S01) outperformed reflective paint (S02) when implemented individually. Deep retrofit (D01) achieved the greatest reduction in overheating intensity, indicating that improvements to the building envelope enhanced the effectiveness of passive cooling strategies, as already observed by Baglivo et al. (2023).

The probabilistic CBA further demonstrated how uncertainty in technical performance propagates into financial outcomes. In the analysed case study, despite substantial reductions in overheating, annual cooling

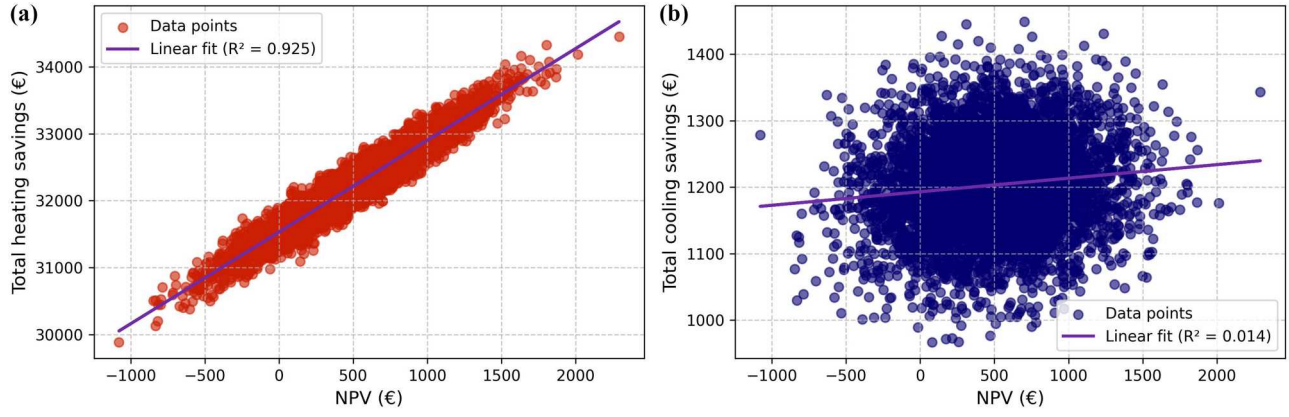


Figure 10. Correlation between the NPV and total heating (a) or total cooling (b) savings for e.g. simple shading retrofit scenario (S01); similar trends are observed for the other scenarios.

cost savings remained below €100 under cooling-only assumptions, resulting in negative NPVs even under the most severe heat scenarios considered. The framework also captured greater variability in financial outcomes for higher-performing passive strategies, with shading (S01) and combined measures (S03) exhibiting wider distributions than reflective paint (S02). Rather than indicating limited technical effectiveness, these results show that operational cooling savings alone are insufficient to recover investment costs for the analyzed building archetype and climatic context. The probabilistic approach therefore provides additional value by quantifying both expected returns and their uncertainty, enabling more transparent assessment of climate-related financial risk.

Integrating heating and cooling demand demonstrated the importance of considering interactions between adaptation and energy-efficiency measures. High-albedo paint increased heating demand, making the shading-only strategy (S01) financially more favourable than the combined strategy (S03). This reflects a broader trade-off where single-aspect improvements create adverse effects (Hamdy et al., 2017; Sheng et al., 2023), similar to how insulation-first retrofits in temperate climates inadvertently increase summer overheating risks (Ibrahim & Pelsmakers, 2018; Liyanage et al., 2024; Yu et al., 2026). Within the analysed Dutch case study, overall financial feasibility remained dominated by heating-related savings, while cooling-related operational savings contributed only marginally, even during annual extremes. Consequently, deep retrofit (D01) emerged as the most financially robust strategy, achieving positive NPVs across all simulations.

Beyond the case study application, the findings also have implications for policymakers developing climate-resilient pathways for buildings. The proposed framework provides a basis for identifying when conventional energy-based assessments may underestimate the benefits of heat resilience measures. This can support retrofit prioritization that accounts for heat risk and inform the development of financial support mechanisms, such as subsidies and incentive schemes, helping to align retrofit investments with resilience objectives.

Limitations & future research

A primary limitation to the presented results is their reliance on a single case study to evaluate retrofit interventions under extreme weather conditions. While the analysed porch house was selected as a representative archetype highly susceptible to overheating within the Dutch housing stock (Hamdy et al., 2017) to demonstrate the framework's application, this fundamentally limits the generalizability of the results. The Dutch building stock encompasses substantial variation in construction periods, envelope characteristics, occupancy patterns, and heating and cooling systems. The insights obtained are therefore bounded to heating-dominated contexts in the Netherlands and similar temperate climates, where financial outcomes remain primarily driven by heating performance. Consequently, the limited cost recovery observed for passive cooling measures should not be interpreted as a general conclusion regarding their economic value, but rather as an illustration of how the framework identifies when heat resilience benefits are missed by conventional energy-based CBA metrics. In climates with longer cooling seasons, higher cooling demand, or more frequent and intense heatwaves, cooling-related savings are expected to become a more influential component of financial feasibility. To ensure the broader transferability of this framework, future research must validate these findings across diverse building typologies, occupant profiles, and cooling configurations. Other significant retrofit interventions should also be considered, such as the use of ceiling fans, personalized environmental control systems for cooling and heating or interventions that can enhance natural ventilation.

Several methodological constraints must also be acknowledged. The definition of 'annual extremes' was derived exclusively by assessing the heat impact on energy demand. However, the worst years for energy consumption do not always coincide with those for thermal comfort, which complicates a standardized definition of extreme years. Furthermore, simulation assumptions regarding ideal HVAC loading, occupant behaviour, and the probability estimation method introduce inherent uncertainties into the results, where sensitivity analysis could clarify their influence. Extending risk assessment for building performance estimation, as proposed by Sun et al. (2016), could help address and quantify such uncertainties. Additionally, the reliance on historical weather data (1995–2024) excludes future climate change trajectories. Future research should integrate predictive models (e.g. IPCC scenarios) to determine if 'heating dominance' persists under sustained warming trajectories, consistent with Baglivo et al.'s (2023) findings for Italy. Beyond future weather scenarios, applying the framework across diverse geographical climatic contexts, similar to the approach of Baglivo et al. (2023), will help identify the specific environmental thresholds where passive cooling measures transition to becoming financially decisive investments. Moreover, accounting for urban

microclimate effects, such as the urban heat island effect and the anthropogenic heat generated by mechanical systems, would also better represent local urban climates (Hamdy et al., 2017).

Finally, the CBA was limited to direct energy costs and static pricing, leaving co-benefits of passive mitigation uncaptured. Future studies could extend the approach by integrating energy price volatility and carbon pricing, as well as the evaluation of the economic damages from extreme heat events. For example, monetizing health through the 'value of statistical life' offers a further potential extension to include thermal comfort outcomes in economic analyses, especially for city-scale (Hyyrynen et al., 2025). Furthermore, including both operational energy emissions and embodied carbon of retrofit materials within multi-criteria decision-making frameworks could provide a more holistic valuation of resilience (Bianchi, 2023).

Conclusion

This study proposes a probabilistic CBA framework that integrates climate uncertainty into retrofit assessment. By characterizing heat extremes as stochastic variables rather than deterministic design scenarios, the framework quantifies climate-induced performance uncertainty and evaluates financial robustness of adaptation strategies under worst-case heat hazard conditions. Applied to a case study building in a temperate climate context, the framework has demonstrated that savings from passive cooling measures are currently insufficient to recover costs. However, the NPV under worst-case conditions exceeded the average NPV, indicating a mitigative effect during extreme events. Furthermore, the local climate conditions resulted in a pronounced asymmetry between heating and cooling demand, amplifying the influence of heating-related measures on overall energy and cost.

The primary contribution of the proposed CBA framework lies in its value for risk-aware decision-making, offering insights into long-term mitigation effects during worst-case hazard recurrence. By capturing the distribution of potential financial outcomes, stakeholders can not only assess the expected economic performance of retrofit strategies but also their robustness under extreme conditions. In practice, this enables stakeholders to identify critical synergistic or counteracting effects between energy domains, such as the potential for passive cooling measures to inadvertently compromise heating efficiency. Ultimately, the framework exposes a performance-domain disparity when applied to the case study: the protective benefits of overheating mitigation vastly outweigh the associated energy cost savings. This demonstrates that in the context of this heating-dominated Dutch residential building, energy savings are a fundamentally inadequate proxy for resilience value. Until cost–benefit assessments explicitly monetize comfort and health, or integrate multi-criteria decision analysis, passive cooling strategies will remain undervalued in similar contexts, leaving occupants vulnerable to a warming climate.

Acknowledgements

This research was funded by the Dutch Research Council (NWO). Diletta Ricci was supported through the NWO–KIC programme Energy Transition as a Socio-Technical Challenge (JUSTPrepare: *Putting Resident Practices and Residential Areas at the Centre of a Just and Effective Energy Transition in Underprivileged Neighbourhoods*, file number KICH1.ED03.20.00). Simona Bianchi was supported by the NWO Talent Programme Veni AES 2023 (Grant Agreement no. 21129) within the project RECLIMATE: *Resource-efficient climate-resilient buildings by multi-hazard risk modelling and resilience-oriented decision making.* Alessandra Luna Navarro has further received funding from the European Union under the Horizon Europe Research & Innovation Programme (101123467 MULTICARE).

Author contributions

CRediT: **Tamara Lalyko:** Conceptualization, Data curation, Formal analysis, Investigation, Methodology, Resources, Software, Validation, Visualization, Writing – original draft; **Diletta Ricci:** Conceptualization, Funding acquisition, Supervision, Writing – original draft, Writing – review & editing; **Simona Bianchi:** Conceptualization, Funding acquisition, Project administration, Supervision, Writing – review & editing; **Alessandra Luna Navarro:** Conceptualization, Supervision, Writing – review & editing.

Disclosure statement

No potential conflict of interest was reported by the author(s).

Funding

This work was supported by HORIZON EUROPE Framework Programme: [Grant Number 101123467]; Nederlandse Organisatie voor Wetenschappelijk Onderzoek: [Grant Number 21129].

Generative AI and AI-assisted technologies in the writing process

When preparing this work, the authors employed Gemini 3 and Grammarly to refine grammar, improve readability and polish the draft. Additionally, GPT-4 was utilized for supervised coding assistance regarding the building performance analysis and the Monte Carlo simulation. All AI-generated output was reviewed and edited by the authors, who maintain full responsibility for the final content.

Data availability statement

The data that support the findings of this study are available at 10.4121/6df3b863-391c-4016-a7fd-3c3bf74111da.

References

ANSI/ASHRAE. (2017). *Standard 55: 2017, thermal environmental conditions for human occupancy*. ASHRAE.

Araújo, C., Almeida, M., Bragança, L., & Barbosa, J. A. (2016). Cost–benefit analysis method for building solutions. *Applied Energy*, *173*, 124–133. https://doi.org/10.1016/j.apenergy.2016.04.005

Archidat Bouwkosten. (n.d.). *Archidat Bouwkosten*. Retrieved May 16, 2025, from https://bouwkosten.archidat.nl/

Baglivo, C., Congedo, P. M., & Malatesta, N. A. (2023). Building envelope resilience to climate change under Italian energy policies. *Journal of Cleaner Production*, *411*, 137345. https://doi.org/10.1016/j.jclepro.2023.137345

Belaïd, F., Ranjbar, Z., & Massié, C. (2021). Exploring the cost-effectiveness of energy efficiency implementation measures in the residential sector. *Energy Policy*, *150*, 112122. https://doi.org/10.1016/j.enpol.2020.112122

Bianchi, S. (2023). Integrating resilience in the multi-hazard sustainable design of buildings. *Disaster Prevention and Resilience*, *2*(3). https://doi.org/10.20517/dpr.2023.16

Binomial test. (2008). *The concise encyclopedia of statistics*. Springer.

Bragolusi, P., & D'Alpaos, C. (2022). The valuation of buildings energy retrofitting: A multiple-criteria approach to reconcile cost-benefit trade-offs and energy savings. *Applied Energy*, *310*, 118431. https://doi.org/10.1016/j.apenergy.2021.118431

Brogno, L, Barbano, F, Leo, L S, & Di Sabatino, S (2025). Review on heatwaves: a risk perspective. *Environmental Research Letters*, *20*(6), 063004. https://doi.org/10.1088/1748-9326/add178.

C3S/ECMWF & WMO. (2026). *European state of the climate* 2025. Copernicus Climate Change Service. https://doi.org/10.24381/zy93-sb27

CBS. (2025). *Eindverbruikersprijzen aardgas en elektriciteit*. StatLine. https://opendata.cbs.nl/statline/#/CBS/nl/dataset/85666NED/table?ts=1742302462137

CIBSE. (2015). *Guide A: Environmental design*. https://www.cibse.org/knowledge-research/knowledge-portal/guide-a-environmental-design-2015

Ebi, K. L., Vanos, J., Baldwin, J. W., Bell, J. E., Hondula, D. M., Errett, N. A., Hayes, K., Reid, C. E., Saha, S., Spector, J., & Berry, P. (2021). Extreme weather and climate change: Population health and health system implications. *Annual Review of Public Health*, *42*(1), 293–315. https://doi.org/10.1146/annurev-publhealth-012420-105026

European Commission. (2015). *Guide to cost-benefit analysis of investment projects – Economic appraisal tool for cohesion policy 2014*-2020. Publications Office of the European Union. https://doi.org/10.2769/97516

Galvin, R. (2024). The economic losses of energy-efficiency renovation of Germany's older dwellings: The size of the problem and the financial challenge it presents. *Energy Policy*, *184*, 113905. https://doi.org/10.1016/j.enpol.2023.113905

Gemeente Rotterdam. (2021). *Rotterdam aardgasvrij – De rotterdamse transitievisie warmte*. https://duurzaam010.nl/content/uploads/2021/06/Rotterdamse-Transitievisie-Warmte-1.pdf

Gemeente Rotterdam. (2024). *Wijkprofiel* 2024 [Dataset]. https://wijkprofiel.rotterdam.nl/nl/2024/rotterdam

Groh, A., Kuhlwein, H., & Bienert, S. (2022). Does energy retrofitting pay off? An analysis of German multifamily building data. *IOP Conference Series: Earth and Environmental Science*, *1078*(1), 012116. https://doi.org/10.1088/1755-1315/1078/1/012116

Guardigli, L., Bragadin, M. A., Della Fornace, F., Mazzoli, C., & Prati, D. (2018). Energy retrofit alternatives and cost-optimal analysis for large public housing stocks. *Energy and Buildings*, *166*, 48–59. https://doi.org/10.1016/j.enbuild.2018.02.003

Guazzi, G., Bellazzi, A., Meroni, I., & Magrini, A. (2017). Refurbishment design through cost-optimal methodology: The case study of a social housing in the northern Italy. *International Journal of Heat and Technology*, *35*(Special Issue1), S336–S344. https://doi.org/10.18280/ijht.35Sp0146

Hamdy, M., Carlucci, S., Hoes, P.-J., & Hensen, J. L. M. (2017). The impact of climate change on the overheating risk in dwellings – A Dutch case study. *Building and Environment*, *122*, 307–323. https://doi.org/10.1016/j.buildenv.2017.06.031

Higney, A., & Gibb, K. (2024). Net zero retrofit of older tenement housing – The contribution of cost benefit analysis to wider evaluation of a demonstration project. *Energy Policy*, *191*, 114181. https://doi.org/10.1016/j.enpol.2024.114181

Hong, T., Malik, J., Krelling, A., O'Brien, W., Sun, K., Lamberts, R., & Wei, M. (2023). Ten questions concerning thermal resilience of buildings and occupants for climate adaptation. *Building and Environment*, *244*, 110806. https://doi.org/10.1016/j.buildenv.2023.110806

Huizenga, C., Zhang, H., Schiavon, S., Kwong, H., Brager, G., Arens, E., Roa, C. D., Exss, K., Lehrer, D., Luna-Navarro, A., Nomoto, A., Ouellet-Plamondon, C., Raftery, P., Sun, R., Thero, R., & Wang, Y. (2024). *Establishing maximum safe indoor temperatures for U.S. residential buildings*. Comfort At The Extremes: Investing in Well-being in a Challenging Future.

Hyyrynen, M., Ollikainen, M., Käyhkö, J., Suomi, J., Lintunen, J., Mäkelä, A., Groundstroem, F. M., & Juhola, S. (2025). Cooling is a cost-efficient way to adapt to heatwaves even in high-latitude cities. *Climatic Change*, *178*(5), 96. https://doi.org/10.1007/s10584-025-03913-8

Ibrahim, A., & Pelsmakers, S. L. (2018). Low-energy housing retrofit in North England: Overheating risks and possible mitigation strategies. *Building Services Engineering Research and Technology*, *39*(2), 161–172. https://doi.org/10.1177/0143624418754386

Johnstone, I. M. (2004). Development of a model to estimate the benefit-cost ratio performance of housing. *Construction Management and Economics*, *22*(6), 607–617. https://doi.org/10.1080/0144619042000202825

KNMI. (2023). *KNMI'23 climate scenarios for the Netherlands KNMI*. De Bilt, KNMI Publication 23-03a. https://cdn.knmi.nl/system/ckeditor/attachment_files/data/000/000/358/original/KNMI23_climate_scenarios_user_report.pdf

KNMI. (n.d.). *Uurwaarden van weerstations*. Koninklijk Nederlands Meteorologisch Instituut. Retrieved May 16,

2025, from https://www.daggegevens.knmi.nl/klimatologie/uurgegevens

Koninklijk Nederlands Normalisatie-instituut. (2017). *NEN-EN 15459-1 – Energieprestatie van gebouwen verwarmingssystemen en op water gebaseerde koelsystemen in gebouwen - deel 1: economische evaluatieprocedure voor energiesystemen in gebouwen, module M1-14*. https://connect.nen.nl/Standard/Detail/3527129?compId=10037&collectionId=0

Krelling, A. F., Lamberts, R., Malik, J., Zhang, W., Sun, K., & Hong, T. (2024). Defining weather scenarios for simulation-based assessment of thermal resilience of buildings under current and future climates: A case study in Brazil. *Sustainable Cities and Society*, *107*, 105460. https://doi.org/10.1016/j.scs.2024.105460

Lassandro, P., & Di Turi, S. (2017). Façade retrofitting: From energy efficiency to climate change mitigation. *Energy Procedia*, *140*, 182–193. https://doi.org/10.1016/j.egypro.2017.11.134

Le, D. M., Christopher, P., & Ngo, T. (2025). Optimising building envelope retrofits under future climates: Integrating passive, active, and renewable strategies. *Case Studies in Thermal Engineering*, *72*, 106219. https://doi.org/10.1016/j.csite.2025.106219

Lee, S. H., Hong, T., Le, M., Medina, L., Xu, Y., Robinson, A., & Piette, M. A. (2024). Assessment of energy and thermal resilience performance to inform climate mitigation of multifamily buildings in disadvantaged communities. *Sustainable Cities and Society*, *104*, 105319. https://doi.org/10.1016/j.scs.2024.105319

Liu, Y., Xue, S., Guo, X., Zhang, B., Sun, X., Zhang, Q., Wang, Y., & Dong, Y. (2023). Towards the goal of zero-carbon building retrofitting with variant application degrees of low-carbon technologies: Mitigation potential and cost-benefit analysis for a kindergarten in Beijing. *Journal of Cleaner Production*, *393*, 136316. https://doi.org/10.1016/j.jclepro.2023.136316

Liyanage, D. R., Hewage, K., Hussain, S. A., Razi, F., & Sadiq, R. (2024). Climate adaptation of existing buildings: A critical review on planning energy retrofit strategies for future climate. *Renewable and Sustainable Energy Reviews*, *199*, 114476. https://doi.org/10.1016/j.rser.2024.114476

Machard, A., Salvati, A., Tootkaboni, P., Gaur, M., Zou, A., Wang, J., Baba, L. L., Ge, F., Bre, H., Bozonnet, F., Corrado, E., Luo, V., Levinson, X., Lee, R., Hong, S. H., Salles Olinger, T., Machado, M., Da Guarda, R. M. E. S., Veiga, E. L. A., … Holzer, P. (2024). Typical and extreme weather datasets for studying the resilience of buildings to climate change and heatwaves. *Scientific Data*, *11*(1), 531. https://doi.org/10.1038/s41597-024-03319-8

Mikulić, D., Bakarić, I. R., & Slijepčević, S. (2016). The economic impact of energy saving retrofits of residential and public buildings in Croatia. *Energy Policy*, *96*, 630–644. https://doi.org/10.1016/j.enpol.2016.06.040

Mirzabeigi, S., Homaei, S., Razkenari, M., & Hamdy, M. (2023). The impact of building retrofitting on thermal resilience against power failure: A case of air-conditioned house. In L. L. Wang, H. Ge, Z. J. Zhai, D. Qi, M. Ouf, C. Sun, & D. Wang (Eds.), *Proceedings of the 5th international conference on building energy and environment* (pp. 2609–2619). Springer Nature.

Nahlik, M. J., Chester, M. V., Pincetl, S. S., Eisenman, D., Sivaraman, D., & English, P. (2017). Building thermal performance, extreme heat, and climate change. *Journal of Infrastructure Systems*, *23*(3), 04016043. https://doi.org/10.1061/(ASCE)IS.1943-555X.0000349

National Research Council. (2012). *Disaster resilience: A national imperative* 2012. The National Academies Press. https://doi.org/10.17226/13457

NCEI. (n.d.). *Data Search*. National Centers for Environmental Information. Retrieved May 16, 2025, from https://www.ncei.noaa.gov/access/search/data-search/global-hourly?stations=06344099999&pageNum=2

NHBC. (2012). *Understanding overheating where to start: An introduction for house builders and designers*. https://www.nhbc.co.uk/binaries/content/assets/nhbc/foundation/understanding-overheating—where-to-start.pdf

NLR. (2023). *OpenStudio* (Version 3.7.0) [Computer software]. https://openstudio.net/news/1700506800

Preciado-Pérez, O. A., & Fotios, S. (2017). Comprehensive cost-benefit analysis of energy efficiency in social housing. Case study: Northwest Mexico. *Energy and Buildings*, *152*, 279–289. https://doi.org/10.1016/j.enbuild.2017.07.014

Ramakrishnan, S., Wang, X., Sanjayan, J., & Wilson, J. (2017). Thermal performance of buildings integrated with phase change materials to reduce heat stress risks during extreme heatwave events. *Applied Energy*, *194*, 410–421. https://doi.org/10.1016/j.apenergy.2016.04.084

Reuters. (2019, September 8). Heatwave caused nearly 400 more deaths in Netherlands: Stats agency. *Reuters*. https://www.reuters.com/article/world/heatwave-caused-nearly-400-more-deaths-in-netherlands-stats-agency-idUSKCN1UZ0GW/

Ricci, D., Konstantinou, T., & Visscher, H. (2025). Making energy renovations equitable: A literature review of decision-making criteria for a just energy transition in residential buildings. *Energy Research & Social Science*, *122*, 104016. https://doi.org/10.1016/j.erss.2025.104016

Rijksoverheid. (n.d.). *EP-Online*. Rijksoverheid. Retrieved May 16, 2025, from https://www.ep-online.nl/

Robert McNeel & Associates. (2023). *Rhinoceros 3D* (Version 8.0) [Computer software].

Ruparathna, R., Hewage, K., & Sadiq, R. (2017). Economic evaluation of building energy retrofits: A fuzzy based approach. *Energy and Buildings*, *139*, 395–406. https://doi.org/10.1016/j.enbuild.2017.01.031

RVO. (2020). *Long-term renovation strategy – En route to a low-CO2 built environment*.

RVO. (n.d.). *Kostenkentallen*. Regelhulpenvoorbedrijven. Retrieved May 16, 2025, from https://regelhulpenvoorbedrijven.nl/kostenkentallen/

Sharbaf, S. A., & Schneider-Marin, P. (2025). Cost-benefit analysis of sustainable upgrades in existing buildings: A critical review. *Energy and Buildings*, *328*, 115142. https://doi.org/10.1016/j.enbuild.2024.115142

Sheng, M., Reiner, M., Sun, K., & Hong, T. (2023). Assessing thermal resilience of an assisted living facility during heat waves and cold snaps with power outages. *Building and Environment*, *230*, 110001. https://doi.org/10.1016/j.buildenv.2023.110001

Spalt, E., Curl, C., Allen, R., Cohen, M., Adar, S., Stukovsky, K., Avol, E., Castro-Diehl, C., Nunn, C., Mancera-Cuevas, K., & Kaufman, J. (2016). Time-location patterns of a diverse population of older adults: The multi-ethnic study of atherosclerosis and air pollution (MESA air). *Journal of*

Exposure Science & Environmental Epidemiology, *26*(4), 349–355. https://doi.org/10.1038/jes.2015.29

Stadsarchief Rotterdam. (n.d.). *Construction plans*. Stadsarchief Rotterdam. Retrieved May 6, 2025, from https://stadsarchief.rotterdam.nl/en/construction-plans

Sun, S., Kensek, K., Noble, D., & Schiler, M. (2016). A method of probabilistic risk assessment for energy performance and cost using building energy simulation. *Energy and Buildings*, *110*, 1–12. https://doi.org/10.1016/j.enbuild.2015.09.070

Sun, Y., Zhu, S., Wang, D., Duan, J., Lu, H., Yin, H., Tan, C., Zhang, L., Zhao, M., Cai, W., Wang, Y., Hu, Y., Tao, S., & Guan, D. (2024). Global supply chains amplify economic costs of future extreme heat risk. *Nature*, *627*(8005), 797–804. https://doi.org/10.1038/s41586-024-07147-z

TABULA WebTool. (2014). TABULA. Retrieved May 16, 2025, from https://webtool.building-typology.eu/#bm

Taylor, J., McLeod, R., Petrou, G., Hopfe, C., Mavrogianni, A., Castaño-Rosa, R., Pelsmakers, S., & Lomas, K. (2023). Ten questions concerning residential overheating in Central and Northern Europe. *Building and Environment*, *234*, 110154. https://doi.org/10.1016/j.buildenv.2023.110154

Vautard, R., Van Aalst, M., Boucher, O., Drouin, A., Haustein, K., Kreienkamp, F., Van Oldenborgh, G. J., Otto, F. E. L., Ribes, A., Robin, Y., Schneider, M., Soubeyroux, J.-M., Stott, P., Seneviratne, S. I., Vogel, M. M., & Wehner, M. (2020). Human contribution to the record-breaking June and July 2019 heatwaves in Western Europe. *Environmental Research Letters*, *15*(9), 094077. https://doi.org/10.1088/1748-9326/aba3d4

Wahi, P., Koster, V., Tenpierik, M. J., Visscher, H., & Konstantinou, T. (2025). A multi-criteria decision-making framework for energy renovations of existing Dutch dwelling. In *Preparing Dutch homes for energy transition: A decision support framework for renovating existing Dutch dwellings for lower temperature district heating* (pp. 221–272). A + BE | Architecture and the Built Environment.

Weglarczyk, S. (2018). Kernel density estimation and its application. *ITM Web of Conferences*, *23*, 00037. https://doi.org/10.1051/itmconf/20182300037

Yu, Q., Mills, G., Ketzler, G., & Leuchner, M. (2026). Summer thermal consequences of EU retrofit strategies: An integrated microclimate and indoor comfort study in Düsseldorf. *Energy and Buildings*, *357*, 117163. https://doi.org/10.1016/j.enbuild.2026.117163

Zhang, C., Kazanci, O. B., Levinson, R., Heiselberg, P., Olesen, B. W., Chiesa, G., Sodagar, B., Ai, Z., Selkowitz, S., Zinzi, M., Mahdavi, A., Teufl, H., Kolokotroni, M., Salvati, A., Bozonnet, E., Chtioui, F., Salagnac, P., Rahif, R., Attia, S., … Zhang, G. (2021). Resilient cooling strategies – A critical review and qualitative assessment. *Energy and Buildings*, *251*, 111312. https://doi.org/10.1016/j.enbuild.2021.111312

Appendix A

Table A.1. Thermal resilience metrics for energy and indoor comfort.

Energy Metrics /Indicators	*Description / Quantification Method*	*Research Purpose*	*References*
Energy Use Intensity /Energy Performance Index	Energy Demand/Use per square meter for a specific period (e.g. average year) [kWh/m² per a]	Testing various retrofitting strategies and measures for building envelopes case study analysis: assisted living facilities; Enhancing building performance prediction with risk modelling	(Baglivo et al., 2023; Lassandro & Di Turi, 2017; Sheng et al., 2023; Sun et al., 2016)
Energy Use/ Demand	annual or additional energy needed for e.g. cooling [kWh]	Analysis of retrofit scenarios on vulnerable multi-family buildings in disadvantaged communities	(Lee et al., 2024)
Primary Energy Demand	annual or additional primary energy depending on energy source & system [kWh]		
Utility Cost, Economic Loss	Expected annual loss or [Euro, Dollar]	Multi-criteria comparison of facade systems in a mediterranean climate; Enhancing building performance prediction with risk modelling	(Bianchi, 2023; Sun et al., 2016)
Expected Carbon Loss	Energy related carbon emissions hazard specific [kg/CO2eq.]	""	(Bianchi, 2023)
Heat Index (HI)	Combines dry-bulb temperature and relative humidity to estimate perceived temperature. Hours are categorized into caution and danger levels using the NOAA/WPC formula.	Quantify indoor heat risk in assisted living and multi-family buildings during extreme heat or cold events with power outages.	(Lee et al., 2024; Sheng et al., 2023)
Hours in Heat Stress	Quantify duration of indoor heat stress exposure. Based on the Standard Effective Temperature (SET); total hours where SET > 30 °C during extreme events.	""	(Lee et al., 2024)
Indoor Overheating Degree (IOD)	Measures intensity and frequency of overheating relative to adaptive comfort limits. Calculated as the hourly sum of the temperature difference between indoor free-running conditions and comfort thresholds (CIBSE: living > 28 °C, bedrooms > 26 °C for > 1 % of occupied hours). Fan use allows + 3 °C adjustment.	Evaluate and compare overheating resilience of Dutch dwellings under current and future climate scenarios.	(Hamdy et al., 2017; Mirzabeigi et al., 2023)

(*Continued*)

Table A.1. Continued.

Energy Metrics /Indicators	*Description / Quantification Method*	*Research Purpose*	*References*
Overheating Escalation Factor	Ratio of indoor to outdoor overheating severity, defined as IOD divided by the ambient warmness degree (average cooling degree hours for $T_o \geq 18$ °C, May–Sept). Values > 1 indicate higher indoor stress.	""	(Hamdy et al., 2017; Mirzabeigi et al., 2023)
Weighted unmet thermal performance (WUMTP)	Multi-zone indicator using fixed comfort limits. Weights indoor temperature deviations by their timing (degradation/ recovery phases), expressed in degree hours or degree hours/m².	Comparing resilience retrofit packages in case of power failure	(Mirzabeigi et al., 2023)
Resilience Class Index	Labeling system A-F based on WUMTP	""	(Mirzabeigi et al., 2023)
Building heat performance index (BHPI)	outlines how fast a building overheats; fixed comfort limit 32°C	Evaluate thermal performance of building archetypes at the urban scale during extreme heat.	(Nahlik et al., 2017)
Temperature Weighted Thermal Performance	Integrates indoor temperature rise over time to characterize the rate and persistence of overheating.	""	(Nahlik et al., 2017)
Metrics based on Discomfort Index: Overheated Hours, hours 80% acceptability not met, severe discomfort hours	Based on the Discomfort Index (average of wet- and dry-bulb temperatures). Classifies mild (< 24 °C), moderate (24–28 °C), and severe (> 28 °C) heat stress. Quantifies hours exceeding 80 % acceptability limits (ASHRAE) using operative temperature.	Evaluate overheating mitigation using Phase Change Materials (PCM) and night cooling strategies.	(Ramakrishnan et al., 2017)

Table A.2. Literature review on CBA for retrofitting.

Reference	*Choosing by Advantages Method*	*Cost-Modelling Method*	*Economic Indicator*	*Analysis Period*	*Savings/ Benefits*	*Key Focus*	*Additional Parameters*
(Araújo et al., 2016)	COA & CBA	Life Cycle Cost	Savings	8 (static payback period)	primary energy demand	Energy Efficiency Technologies	investment willingness for sustainable solutions
(Bragolusi & D'Alpaos, 2022)	CBA	Incremental Cost	NPV	30	Energy	/	/
(Guardigli et al., 2018)	COA & CBA	Global Cost	NPV, PP	30	energy	Cost optimal of envelope retrofits	global cost for 10/ 20/30 years, annual savings per m²
(Guazzi et al., 2017)	COA	Global Cost	PP, Eur/m²a to kWh/m²a	30	energy performance	/	Final Value/ Residual Value
(Galvin, 2024)	CBA	IC, EC & "Anyway" Cost	NPV	25	energy	energy retrofitting	prebound and Rebound Effects, incl. anyway costs, investment as loan
(Higney & Gibb, 2024)	social CBA	Mix, IC, MC, Administrative Cost, EC	NPV, BCR	30, 20 (EU)	energy, carbon	incl. non-market values & behavioural response	embodied carbon cost factor included
(Hyyrynen et al., 2025)	CBA	Investment costs, Operational costs	NPV	78 years (2022-2100)	Reduced mortality risk	Mitigating overheating with mechanical cooling	Value of statistical life
(Johnstone, 2004)	CBA	Life Cycle Cost	BCR	Specific component life cycle	*unknown*	population dynamics, housing typologies	/
(Liu et al., 2023)	CBA, CEA	Life cycle incremental cost	Total Cost, NPV, incremental cost-effectiveness ratio	*Full building life cycle 50 years*	energy efficiency, carbon & cost	carbon emission reduction	/
(Mikulić et al., 2016)	CBA	Investment costs	NPV, savings comparison	20	energy, economic activity, fiscal impact, environmental impact	socio-economic impact of energy renovation	Social benefits

Appendix B

Retrofit scenarios global costing and cost-benefit analysis inputs

Table B.1. Costs of retrofit measures: investment (IC), maintenance (MC), replacement (RC) (Archidat Bouwkosten, n.d.; RVO, n.d.).

District Heating IC	Connection Cost	8	households	1,518.62	per unit	12,188,96	**12,190.00**	**Euro**
Shading IC	*All southern openings*					8,303.40	**8,300.00**	**Euro**
	Awning w:1000mm	12	pcs	329.05	Per piece	3,948.60		
	Awning w:3000mm	8	pcs	544.35	Per piece	4,354.80		
Shading MC	Repair cost	36	m	13.10	Per m	471.60	**470**	**Euro**
	Cycle (warranty)						**5**	**Years**
Shading RC	Life span						**30**	**Years**
Paint	*Full southern facade*					5,953.11	**6,000.00**	**Euro**
	Painting	136.5	m^2	40	Per m^2	5,460.00		
	Scaffolding for 1 week	34	m^2	14.45	Per m^2	493.11		
Paint RC	Life span						**15**	**Years**
Windows IC	*Retrofit all windows to double-glazed*					42,714.18	**42,700.00**	**Euro**
	PVC; 2-division; 1000x1450	14	pcs	711.02	Per piece	9,954.28		
	PVC; 3-division; 1800mm	16	pcs	646.15	Per piece	10,338.40		
	PVC; double doors; 1800mm	6	pcs	2268.33	Per piece	13,609.98		
	PVC; one door; 900mm	8	pcs	1101.44	Per piece	8,811.52		
Façade IC	*Exterior insulation*					41,488.56	**41,500.00**	**Euro**
	140mm mineral wool incl. stucco	256.6	m^2	130.7	Per m^2	33,537.62		
	Scaffolding for 4 weeks	388.5	m^2	15.35	Per m^2	5,963.48		
	Street Protection Net	194.25	m^2	0.5	Per m^2	97.13		
	Windowsills PVC 1000mm	14	m	34.08	Per m	477.12		
	Windowsills PVC 2000mm	33.6	m	42.06	Per m	1.413,22		

Table B.2. Data inputs and analysis settings for the cost-benefit analysis.

Analysis Settings	
Start Year	2025
Analysis Period	30 years
Discount Rate	3%
Number of CBA simulations	5,000
Number of savings samples	10,000
Universal Data	
Variable Electricity Price	0.243 Euro/kWh
Variable Gas Price	0.1604 Euro/kWh
Fixed Gas Price	247.16 Euro
Variable District Heating Price	0.168 Euro/kWh
Fixed District Heating Price	291.42 Euro
Efficiency Air-conditioning	2.9
Efficiency Gas-boiler	0.85
Efficiency District Heating	1.0

Heating only building performance assessment and cost-benefit analysis

Table B.3. Heating Demand Percentiles and Matching Reference Years.

Percentile	***Total Annual Demand [kWh]***	***Closest Matching Year***	***Total Annual Demand [kWh]***	***Corresponding Actual Percentile***
Minimum (0)	57,970.44	2023	57,970.44	0
5	60,206.59	1995	61,731.36	11
25	64,468.82	2018	64,480.99	25
50	68,669.76	2019	6,832.23	51
75	72,675.98	2012	68,769.56	75
95	76,654.87	2011	77,030.71	96
Maximum (100)	78,200.05	2010	78,200.05	100

Table B.4. Building performance and NPV results for heating retrofit assessment.

Scenario	***Baseline***	***S01 shading***	***S02 paint & S03 combi***	***M01 shading***	***D01 shading-paint***
Heating Energy Use Mean [kWh/m²]	161 kWh/m^2	136.5 kWh/m^2	142.3 kWh/m^2	119.0 kWh/m^2	74.8 kWh/m^2
Heating Energy Use StD [kWh/m²]	13.17 kWh/m^2	11.18 kWh/m^2	11.99 kWh/m^2	10.31 kWh/m^2	7.76 kWh/m^2
Heating Cost Savings Mean [€]	/	€1,382.7	€ 895.3	€2,881.8	€6,634.0
NPV Mean [€]	/	€9,522.72	€205.03	€-2,712.76	€29,933.44
Standard Deviation [€]	/	€425.36	€214.98	€761.39	€1,329.93
NPV Confidence Interval 95% [€]	/	8,725.00 to 10,376.70	−213.46 to 633.70	−4,190.55 to −1,236.16	27,384.08 to 32,559.34
% of Negative Values	/	0.00%	16.70%	99.96%	0.00%